ISTANBUL TECHNICAL UNIVERSITY ★ GRADUATE SCHOOL

AMPS-BASED H-BONDED SUPERABSORBENT HYDROGELS

M.Sc. THESIS

BÜŞRA SEKİZKARDEŞ

Department of Chemistry

Chemistry Programme

JUNE 2023

ISTANBUL TECHNICAL UNIVERSITY ★ GRADUATE SCHOOL

AMPS-BASED H-BONDED SUPERABSORBENT HYDROGELS

M.Sc. THESIS

BÜŞRA SEKİZKARDEŞ
(509201204)

Department of Chemistry

Chemistry Programme

Thesis Advisor: Prof. Dr. Oğuz OKAY

JUNE 2023

İSTANBUL TEKNİK ÜNİVERSİTESİ ★ LİSANSÜSTÜ EĞİTİM ENSTİTÜSÜ

AMPS-TABANLI H-BAĞLI SUPERABSORBAN HİDROJELLER

YÜKSEK LİSANS TEZİ

BÜŞRA SEKİZKARDEŞ
(509201204)

Kimya Anabilim Dalı

Kimya Programı

Tez Danışmanı: Prof. Dr. Oğuz OKAY

HAZİRAN 2023

Büşra SEKİZKARDEŞ, a M.Sc. student of ITU Graduate School student ID 509201204, successfully defended the thesis entitled "AMPS-BASED H-BONDED SUPERABSORBENT HYDROGELS", which she prepared after fulfilling the requirements specified in the associated legislations, before the jury whose signatures are below.

Thesis Advisor :	**Prof. Dr. Oğuz OKAY** Istanbul Technical University	.....
Jury Members :	**Doç. Dr Bünyamin KARAGÖZ** Istanbul Technical University	.....
	Dr. Esra SU Istanbul University	.....

Date of Submission : 19 May 2023
Date of Defense : 7 June 2023

To my family,

FOREWORD

First of all, I would like to thank to my supervisor Prof. Dr. Oğuz OKAY for giving me the chance of pursuing science by his side. His guidance, patience, and support have been important driving forces behind the development of this study. He will stay as one of the most influential people in my life and as a scientist, I will try to take my cue from him. There are no words to express my gratitude to my advisor for accepting my request of attending his research group.

I am forever indebted to my mentor Dr. Esra SU. She made my journey far more easy. I was very lucky to work with her. I am grateful to her and the time that she spent helping me on many occasions.

Thanks to lab members of Polymeric Gels Research Lab. Ç. Buse Oral, Gamze Gerim, Gamze Döşer, Sümeyye Özer, and Çağla Erkoç.

I would like to thank my best friend Berk Aytaç for being by my side since the first week of high school.

Best wishes and thanks to my friends Adalet Nur Kaya, İpek Kayalı, and Şevval Demirkan who are continuing their master's studies at Istanbul Technical University.

My family has always been my biggest strength. I am grateful for their support and love. The most precious person in my life is my sister Zehra. I am so blessed to have a little sister like her, she is my hope when I am at a loss. I would like to thank her for being my source of happiness.

I would like to express my gratitude to my professors Prof. Dr. Dolunay Şakar Daşdan and Prof. Dr. M. Kasım Şener for their references and support on my application to the Graduate School of ITU.

Finally, I would like to thank the Scientific and Technical Research Council of Turkey-Directorate of Science Fellowships and Grant Programmes (TUBITAK BIDEB) for 2210-A National Scholarship for MSc Students 2020/2.

June 2023

Büşra SEKİZKARDEŞ
Chemist

TABLE OF CONTENTS

Page

ABBREVIATIONS

3D	**:** Three-dimensional
AAc	**:** Acrylic acid
AMPS	**:** 2-acrylamido-2-methylpropane sulfonic acid
ATR-FTIR	**:** Attenuated total reflectance-Fourier transform infrared
CD	**:** Cyclodextrins
DAT	**:** Diaminotriazine
DMAA	**:** N,N-dimethylacrylamide
DOPA	**:** 3,4-dihydroxyphenylalanine
HA	**:** Hyaluronic acid
Irgacure	**:** 2-Hydroxy-4′-(2-hydroxyethoxy)-2-methylpropiophenone
kPa	**:** Kilopascal
LCST	**:** Lower critical solution temperature
LVR	**:** Linear viscoelastic regime
MAAc	**:** Methacrylic acid
MPa	**:** Megapascal
MPTC	**:** 3-(Methacryloylamino)propyl]trimethylammonium chloride
NaSS	**:** Sodium p-styrenesulphonate
NPMA	**:** 4-nitrophenyl metacrylate
NPMAAHG	**:** Poly(nitrophenyl methacrylate-co-methacrylic acid)
PAAm	**:** Poly(acrylamide)
PAMPS	**:** Poly(AMPS)
PEG	**:** Polyethylene glycol
PNIPAm	**:** Poly(N-isopropylacrylamide)
PVDT	**:** Poly(2-vinyl-4,6-diamino-1,3,5-triazine)
SAPs	**:** Superabsorbent polymers
TEMED	**:** N,N,N',N'-tetramethylethylenediamine
UPy	**:** Ureidopyrimidinone
UV	**:** Ultraviolet
C17.3	**:** Stearyl methacrylate
C22	**:** Dococyl acrylate

SYMBOLS

ε	: Strain
ε_f	: Strain at break
$\dot{\varepsilon}$	: Strain rate
λ	: Deformation ratio
λ_{biax}	: Biaxial extension ratio
λ_f	: Deformation ratio at break
$\dot{\gamma}$	: Shear rate
γ_{cr}	: Critical strain
γ_o	: Strain amplitude
η	: Viscosity
σ_f	: Fracture stress
σ_{nom}	: Nominal stress
σ_{true}	: True stress
σ_y	: Yield stress
ω	: Angular frequency
ω_c	: Crossover frequency
x_{MAAc}	: Mol fraction of MAAc
a_s	: Expansion ratio
C_o	: Monomer concentration
E	: Young's Modulus
E_a	: Activation energy
f_{diss}	: Ratio of dissipated energy
G'	: Elastic/strorage modulus
G''	: Viscous/loss modulus
G_o	: Linear modulus
m_{dry}	: Weight of gels in dry state
m_o	: Weight of gels after preparation
m_{rel}	: Equilibrium relative weight swelling ratio
q_w	: Equilibrium weight swelling ratio in dry state
R_o	: End-to-end distances of the chains in as-prepared hydrogel

R_s : End-to-end distances of the chains in swollen hydrogel

$\tan \delta$: Loss factor

U_{hys} : Hysteresis energy

v_e : Volume fraction of gel in equilibrium with water

$v_{e,chem}$: Cross-link density of chemical

V_a : Activation volume

W : Toughness

W_g : Gel fraction

LIST OF TABLES

Page

LIST OF FIGURES

Page

AMPS-BASED H-BONDED SUPERABSORBENT HYDROGELS

SUMMARY

Water is the most abundant molecule in living tissues, and organisms. The presence of soluble ions and water provides regulation, protection, and conductivity to the nature of the systems. Different bodily parts store varying amounts of water according to their place and duty. The bones and teeth contain the lowest percentage of water in the body, whereas the brain and kidneys have the highest percentage. Materials that resemble the mechanical properties and behavior of biological tissues are now possible thanks to new polymeric networks. The distinctive qualities of hydrogels, like their high water content, softness, and flexibility that can mimic those of human tissues and organs, as well as biocompatibility have made them particularly desirable.

These properties can be tailored according to the purposed area however poor mechanical properties restrict the efficient application of the hydrogels. Many hydrogel network structures, such as double network hydrogels, macromolecular microsphere composite hydrogels, physically cross-linked networks, and nanocomposite hydrogels, have been produced to address this issue.

The objective of this study is to prepare hydrogels that could absorb a high amount of water without compromising their structural integrity and exhibit desirable mechanical characteristics (such as high stiffness, and toughness). Particularly strong, dynamic hydrogels can be obtained by using physical crosslinks in the hydrogel network structure which give an energy dissipation mechanism to avoid fracture and gain reversibility under stress.

Today many studies are inspired by the mechanical features and high water content of biological tissues for the preparation of hydrogels. Because macromolecules naturally interact with one another through noncovalent interactions, supramolecular assemblies are frequently found in biological systems.

The hydrogels based on 2-acrylamido-2-methyl-1-propanesulfonic acid (AMPS) have enormous and pH-independent water absorption capacity and electro-sensitive characteristics when swollen in water. Because they are frequently produced using chemical cross-linkers, their network structures cannot effectively dissipate energy and poly(AMPS) (PAMPS) hydrogels with poor mechanical properties are obtained. A physically crosslinked dynamic PAMPS network dissipating energy under stress can be made by replacing chemical crosslinks with cooperative H-bonds to improve mechanical properties.

Multiple H-bonding interactions are necessary for the creation of strong physical hydrogels that are stable in water. Therefore, careful consideration must be given while choosing monomers that will form cooperative H-bonds. Preliminary experiments were conducted with N,N-dimethylacrylamide (DMAA), methacrylic acid (MAAc), and acrylic acid (AAc) to investigate comonomer effect. Because AMPS/DMAA and AMPS/MAAc copolymer hydrogels have good mechanical properties and the carbonyl of DMAA and the carboxyl group of MAAc are known to produce multiple H-bonds connecting primary polymer chains, AMPS/MAAc/DMAA terpolymer

hydrogels were prepared without using any chemical cross-linker. Effect of terpolymer composition was investigated by preparing hydrogels at various MAAc/DMAA molar ratio at a constant water content (w) of 25 wt%. The terpolymer hydrogels exhibited the best mechanical properties at a MAAc/DMAA molar ratio of 4:1 (x_{MAAc} = 0.8).

Then, by fixing the MAAc/DMAA molar ratio at 4:1, we increased the water content (w) from 25 to 95 wt% to observe the effect of water amount at gelation on the hydrogel properties. Visual inspection showed that the transparent terpolymer hydrogels formed at a water content lower than 40 wt% become translucent at 50 wt%, and finally opaque at 75 wt%. A phase-separated system formed of a viscous solution and an opaque gel was obtained by further increasing the water content w to 93 wt%. Both fracture stress σ_f and the modulus E three orders of magnitude decrease (from 26±2 MPa to 7±1 kPa, and 10.4±0.7 MPa to 15±1 kPa, respectively) with increasing w from 25 to 75 wt%.

Detailed studies revealed the formation of cooperative H-bonds that link MAAc and DMAA segments leading to a phase separation of the highly H-bonded regions. Their network structure is characterized by rheological tests, FTIR, and elemental analyzes. Furthermore, swelling tests also showed that the superabsorbent behavior of AMPS-based terpolymer hydrogels was improved by the addition of comonomers to the structure. In short, better mechanical strength and high water absorption were obtained by the addition of comonomers MAAc and DMAA to the AMPS hydrogel network structure.

AMPS-BAZLI H-BAĞLI SÜPERABSORBAN HİDROJELLER

ÖZET

Su, canlı dokularda ve organizmalarda en bol bulunan moleküldür. Çözünür iyonların ve suyun varlığı, sistemlerin doğasına düzenleme, koruma ve iletkenlik gibi özellikler sağlamaktadır. Vücudun farklı bölümleri, bulundukları yere ve işlevlerine göre değişen miktarlarda su içermektedir. Kemikler ve dişler vücuttaki en düşük su yüzdesini içerirken, beyin ve böbrekler en yüksek yüzdeye sahiptir. Polimerik ağ yapılar sayesinde biyolojik dokuların mekanik davranışlarını taklit eden malzemelerin eldesi artık mümkündür. Hedeflenen alana göre ayarlanabilen; yüksek su içeriği, yumuşaklık ve insan doku ve organlarına benzeyen esneklik gibi özelliklerin yanında biyouyumluluk hidrojelleri ilgi çekici hale getirmiştir ancak zayıf mekanik özellikler hidrojellerin pratik uygulamasını kısıtlamaktadır. Bu sorunu çözmek adına çift ağ yapılara sahip hidrojeller, makromoleküler mikroküreler içeren kompozit hidrojeller, nanokompozit hidrojeller ve fiziksel çapraz bağlı hidrojeller dahil olmak üzere farklı hidrojel ağ yapıları oluşturulmuştur. Hidrojel ağ yapısında bulunan fiziksel çapraz bağlar yapıya enerji dağıtım mekanizması sağlar, stres altında kırılmayı önler; böylece özellikle güçlü, dinamik hidrojeller elde edilebilir.

Bu çalışmanın amacı yapısal bütünlüklerini koruyarak yüksek miktarda su absorplayan ve yüksek sertlik, tokluk gibi mekanik özelliklere sahip fiziksel çapraz bağlı hidrojeller elde etmektir.

Günümüzde birçok çalışma, hidrojellerin hazırlanması için biyolojik dokuların mekanik özelliklerinden ve yüksek su içeriğinden ilham almıştır. Makromoleküller, kovalent olmayan etkileşimler yoluyla doğal olarak birbirleriyle etkileşime girdiğinden, biyolojik sistemlerde supramoleküler birleşmeler sıklıkla bulunmaktadır.

2-akrilamido-2-metil-1-propansülfonik asit (AMPS) bazlı hidrojeller, suda şiştiklerinde elektro-duyarlılık ve muazzam pH'dan bağımsız su emme kapasitesine sahiptir. Üretimleri sırasında kovalent çapraz bağlayıcıların sıklıkla kullanılması nedeniyle ağ yapıları enerjiyi etkin bir şekilde dağıtamaz ve zayıf mekanik özelliklere sahip poli(AMPS) (PAMPS) hidrojeller elde edilir. Yüksek mekanik dayanıma sahip, fiziksel çapraz bağlı, dinamik yapıda, enerji dağıtımı yapabilen PAMPS ağ yapısı elde edilmesi; kimyasal çapraz bağları, kooperatif hidrojen bağları ile değiştirmekle mümkündür. Suda kararlı olan güçlü fiziksel hidrojellerin oluşturulması için polimer zincirleri arasında çoklu H-bağ etkileşimleri gereklidir. Bu nedenle, kooperatif H-bağları oluşturacak monomerler seçilirken dikkatli olunmalıdır. Bu çalışmada komonomer etkisini araştırmak için N,N-dimetilakrilamid (DMAA), metakrilik asit (MAAc), akrilik asit (AAc) ile ön deneyler yapılmıştır. AMPS/DMAA ve AMPS/MAAc kopolimer hidrojelleri iyi mekanik özelliklere sahip olduğundan ve DMAA'nın karbonil grubu ile MAAc'nin karboksil grubunun kopolimer zincirleri arasında çoklu H-bağları oluşturduğu bilindiğinden, AMPS/MAAc/DMAA terpolimer hidrojelleri herhangi bir kimyasal çapraz bağlayıcı kullanılmadan hazırlanmıştır. Çeşitli MAAc mol kesirlerinde hidrojeller hazırlanılarak, komonomer konsantrasyonunun etkisi araştırılmıştır. Bu numunelere uygulanan çekme testlerinin

sonucunda terpolimerin, 4:1 MAAc/DMAA mol kesrinde (x_{MAAc}= 0.8) en iyi mekanik özelliklere sahip olduğu tespit edilmiştir. Ardından, seyreltilmiş hidrojel sistemindeki değişiklikleri incelemek için sabit x_{MAAc}= 0.8'de su miktarı (w) ağırlıkça % 25 ve % 95 arasında değiştirilmiştir. Görsel gözlem, ağırlıkça $w \leq$ % 40'ta saydam hidrojellerin oluştuğunu, ağırlıkça %50'de yarı saydam hale geldiklerini ve son olarak ağırlıkça %75'te opak görünüme sahip olduklarını ortaya çıkardı. Su miktarında (w) daha fazla artış ağırlıkça $w \geq$ % 93'te, viskoz bir çözelti ve opak jelden oluşan faz ayrımlı bir sistemle sonuçlandı. Değişen su içeriklerine sahip hidrojellerin dış görüntüsünde gözle görülür farkların olması, jelleşme sırasında oluşan ağ yapının da farklı olduğuna işaret etmektedir. Su içeriğinin ağırlıkça %25'ten %75'e çıkarılmasıyla hem modül E hem de kırılma gerilimi σ_f sırasıyla 26±2 MPa'dan 7±1 kPa'ya ve 10,4±0,7 MPa'dan 15±1 kPa'ya olacak şekilde azalır.

Tüm hidrojeller suda kararlı kalmalarına rağmen, H-bağlı fiziksel yapılarından dolayı üre çözeltilerinde 2 hafta içinde kolaylıkla çözünürler. Suyla diyaliz edilerek ürenin uzaklaştırılması sonrası ağırlıkça %4 PEG-10000 çözeltisine karşı diyaliz edilip, liyofilizatörle kurutularak izole edilen terpolimerlerin ağırlıkça %1'lik sulu çözeltisiyle reolojik testler yapılmıştır. Elde edilen hidrojel çözeltileriyle kayma hızına karşı viskozite ölçümleri ve frekans taramaları yapılmıştır. Çözeltilerinin viskozite ölçümü jelleşmede daha yüksek monomer konsantrasyonunda daha uzun birincil zincirlerin oluşumunu göstermiştir. Yani, w ne kadar düşükse, çözelti viskozitesi o kadar yüksek olmaktadır. Yapılan frekans taramalarındaysa yarı seyreltik polimer çözeltilerinde gözlemlenebilen, çakışma noktaları ($G' = G''$) incelenmiştir. G'', düşük frekanslarda G' aşarken, artan frekansla G' ve G'' arasında çakışma noktası gözlemlenmektedir. Yani frekans yükseldikçe hidrojeller sıvı benzeri davranıştan katı benzeri davranışa geçmektedir. w ağırlıkça %75'ten %25'e düşerken geçiş frekansı ω_c 26'dan 15 s^{-1}'e düşer. Dolayısıyla bu sonuçlar saydam jellerin opak jellere göre daha uzun zincirli ve daha çok moleküller arası hidrojen bağı içerdiğine işaret etmektedir. Artan su içeriği ile önce opaklığın ve nihayet faz ayrımının ortaya çıkması, MAAc ve DMAA birimleri arasında güçlü H-bağlı komplekslerin hidrojeldeki tüm suyu tutamamasıyla açıklanabilmektedir. Yüksek oranda H-bağı içeren ve dolayısıyla fiziksel olarak yüksek oranda çapraz bağlı bölgelerin su emme kapasitesi, gevşek çapraz bağlı bölgelere göre daha düşük olacağından, jel fazının çözelti fazından ayrılması söz konusudur. Bu davranış, w = % 95 'te oluşan hidrojel için açıkça gözlenmiş ve her iki fazın da kompozisyonunu açığa çıkarmak için liyofilizatörde kurutulan örneklere FTIR analizi yapılmıştır. FTIR spektrumunun amid I bölgesinde (dalga boyu) yapılan analiz, çözelti (sol) fazının AMPS birimlerince zengin olduğunu, MAAc birimlerinin ise jel fazında yoğun olduğunu ortaya koymaktadır. Ağırlıkça w = % 93 ve % 95'te oluşan hidrojellerinin her iki fazına da karbon, azot ve kükürt (C, N ve S) için elementel analiz yapılmıştır.

Ayrıntılı çalışmalar, MAAc ve DMAA üniteleri arasında, yüksek oranda H-bağlı bölgelerin faz ayrımına yol açan kooperatif H-bağlarının oluşumunu ortaya çıkarmıştır. Sentezlenen hidrojellerin ağ yapıları reolojik testler, FTIR ve elementel analizler ile karakterize edilmiştir.

Şişme testleri AMPS bazlı kopolimer ve terpolimer hidrojellerin süper emicilik özelliğinin, yapıya komonomerlerin eklenmesinden etkilenmediğini göstermiştir. Farklı x_{MAAc} değerlerinde sentezlenen hidrojellerin kuvvetli polielektrolit olan AMPS birimleri sayesinde sentez sonrası durumlarına göre 1700 - 2900 kat şiştikleri görülmüştür. Jel kesirleri de (W_g) 0.64 - 0.94 aralığındadır ve jellerin 2 ay boyunca bol su içerisinde çözünmeden formlarını koruyabildikleri gözlemlenmiştir. Kısacası,

AMPS hidrojel ağ yapısına MAAc ve DMAA komonomerlerinin eklenmesiyle daha iyi mekanik mukavemet ve yüksek su emme kapasitesi elde edilmiştir.

1. INTRODUCTION

Hydrogels are composed of three-dimensional crosslinked hydrophilic polymer networks. The main property of hydrogels is absorbing and retaining extensive amounts of aqueous solutions with preserving their own structural integrity.

Superabsorbent polymers, a group of materials that could store large quantities of water (at least more than 100 times) without dissolving, first appeared in the 1950s [1]. In response to the great need for superabsorbent materials for hygiene applications, superabsorbent material research has advanced rapidly in recent decades. However, superabsorbent hydrogels are also likely to be used in numerous industries, including agriculture, drug delivery, wastewater treatment, and sanitary products [2–5]. Their biodegradability, outstanding swelling capacity, and good water-retaining ability make them possible candidates for these areas.

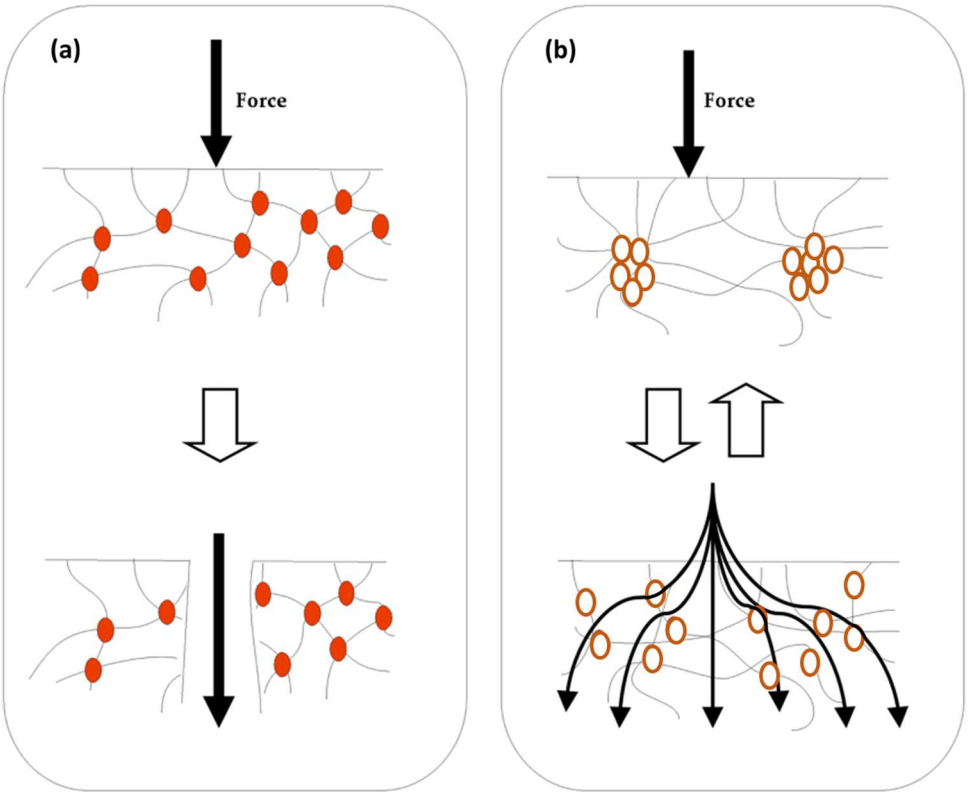

Figure 1.1 : Cartoons demonstrating (a) fracture of a chemically cross-linked hydrogel as a result of the fracture energy localization and, (b) dissipation of the fracture energy in a physically cross-linked hydrogel [9].

2-Acrylamido-2-methylpropane sulfonic acid (AMPS) is a well-known monomer to obtain superabsorbent hydrogels used in baby diapers, agriculture and biomedical fields like wound dressing, drug delivery systems. However, poly(AMPS) (PAMPS) hydrogels usually exhibit weak mechanical performance because of their chemically crosslinked structure, limiting their areas of usage [6–8]. As reported before and schematically illustrated in Figure 1.1 under stress, chemically cross-linked hydrogels behave as a brittle material, while physical ones behave as a tough material due to the dissipation of energy from the hydrogel network [9].

New generation hydrogels with exceptional mechanical properties, comparable to tissues that can bear load including connective tissues like cartilage, and ligaments, have been created in recent years by using the energy dissipation mechanism [10–17]. H-bonding is a significant form of supramolecular interaction that can be used to create dynamically organized physical hydrogels with self-healing and self-recovery behavior without breaking under stress. Multiple H-bonds can easily form between H-bonding acceptor and donor functional sites of polymer chains by yielding extraordinary mechanical strength.

In our previous studies, we have shown that the UV polymerization method can be used in the synthesis of hydrogels that only have physical crosslinks [18]. In addition, the same study showed that by choosing N,N-dimethylacrylamide (DMAA) as a comonomer alongside AMPS, the complementary H-bonds required to create self-healing and shape-recovery properties can also be created. The objective of this study was to understand how the mechanical behaviour of superabsorbent AMPS/DMAA hydrogels varies by replacing the DMAA with the combination of DMAA and methacrylic acid (MAAc), which are H-bond donor and H-bond acceptor units, respectively. We prepared hydrogels at various MAAc/DMAA mol ratios and water contents. As will be seen, AMPS/MAAc/DMAA terpolymer hydrogel prepared at a MAAc/DMAA mol ratio of 4:1 (x_{MAAc} = 0.8) exhibit 63-fold higher modulus (26 vs 0.41 MPa) as compared to AMPS/DMAA hydrogel. When we increased the water content w from 25 to 95 wt% at x_{MAAc} = 0.8 there is a transition in appearance from transparent to opaque indicating the formation of highly H-bonded aggregates. Moreover, results obtained from rheological tests, FTIR, and elemental analyzes can be explained by the changes in the density and strength of H-bonded regions depending

on the water content. With increasing water content, the number of cross-link domains decreases due to the formation of highly H-bonded interconnected regions.

2. LITERATURE

2.1 Hydrogels

Hydrogels consist of crosslinked polymer chains that can swell in water without dissolving. The water-absorbing property of hydrogels is mainly bacause of hydrophilic groups, while dissolution resistance is due to cross-links between chains. Cross-linking in hydrogels also provides the necessary mechanical endurance and physical consistency. Thus, hydrogels can absorb water or biological fluids which is thermodynamically compatible with the nature of the hydrogel without dissolving and swollen.

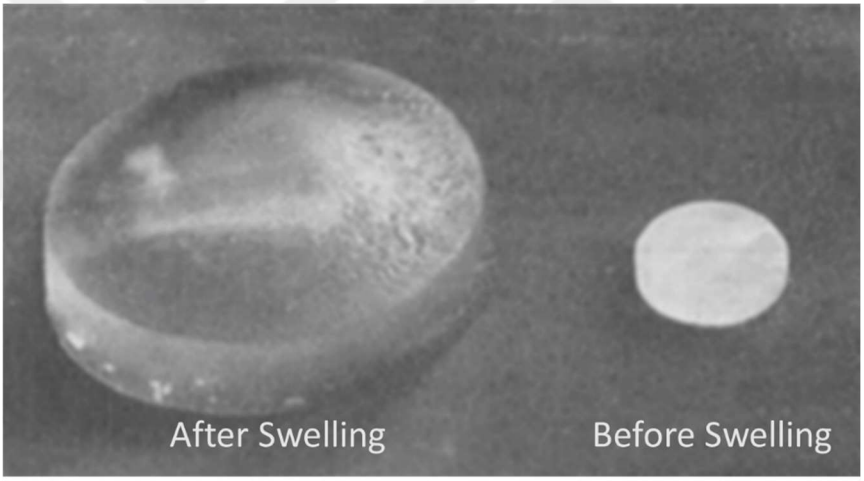

Figure 2.1 : The images of Staudinger's polystyrene gels before and after swelling in benzene [19].

While scientists could make polymers, there was no explanation about how they were formed until 1922. Staudinger was the first scientist who made the definition of polymers and proposed the name of macromolecules [20]. Figure 2.1 shows the image of the first reported gel in 1935 by Staudinger, which is a benzene-swollen polystyrene gel cross-linked with divinylbenzene [19]. Theoretical foundations of gel formation and characteristics were later defined by Flory [21]. The possibility of dramatic volume variations in hydrogels in response to a particular external stimulant was first proposed by Dusek and Patterson [22]. Numerous polymers were identified as responsive to changes in temperature, pH, and pressure, as well as to irradiation,

electric fields, and chemical potential after the discovery of smart hydrogels by Tanaka in the late 1970s [23]. This response caused by the changes of environmental intensive variables can be a minor change as well as a total collapse or inversion of their properties such as volume. The volume phase transition of a temperature-responsive hydrogel can be seen in Figure 2.2 [24]. Unlike most hydrogels, solubility of the hydrogel sharply decreases above the lower critical solution temperature (LCST) in water and the LCST of a polymer mostly influenced by hydrophilic and hydrophobic content within the polymer. Poly(N-isopropyl acrylamide) (PNIPAm) is the best example of a thermoresponsive smart polymeric material with well-understood properties [25]. Hydrophobic and hydrophilic chemical groups are both present in the polymer PNIPAM. At temperatures lower than 32 °C, the hydrophilic amide groups are able to establish hydrogen bonds. At 32 °C the hydrophobic isopropyl group dominates causing the polymer to separate from the aqueous phase. An enormous amount of interest has been sparked by these developments and discoveries in theoretical and experimental studies on hydrogels alongside their applications in industry.

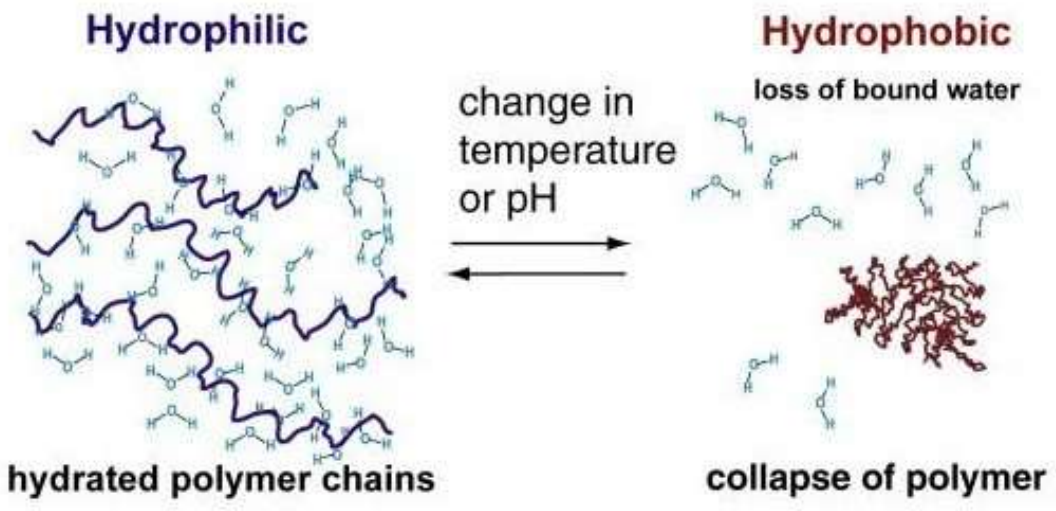

Figure 2.2 : Temperature-dependent inverse solubility characteristics of responsive polymers at the LCST. Hydrated polymer chains below LCST (left) and the collapse of polymer above LCST (right) as a result of entropic water loss with the effect of stimuli [24].

2.2 Macromolecular Hydrogels

Hydrogels are adaptable scaffold materials with qualities that can be tailored to the needs of the target region. By chemical or physical crosslinking, hydrogels have been produced using a variety of polymers, such as synthetic, natural, and also hybrid polymers that contain both natural and synthetic components. Hydrogels resemble natural soft tissues because they are responsive to stimuli and have a high-water absorption. Therefore, they have a variety of applications, such as in biomedical fields like tissue engineering, artificial organs, medication delivery systems, and contact lenses as well as actuators and sensors [6,26–29]. However, tough hydrogels have recently been developed and mechanical properties improved.

Physical hydrogels are reversibly bound by molecular entanglements or non-covalent forces like ionic interactions, H-bonds, and hydrophobic interactions. On the contrary, irreversibly cross-linked hydrogels via covalent forces are considered "chemical" (Figure 2.3).

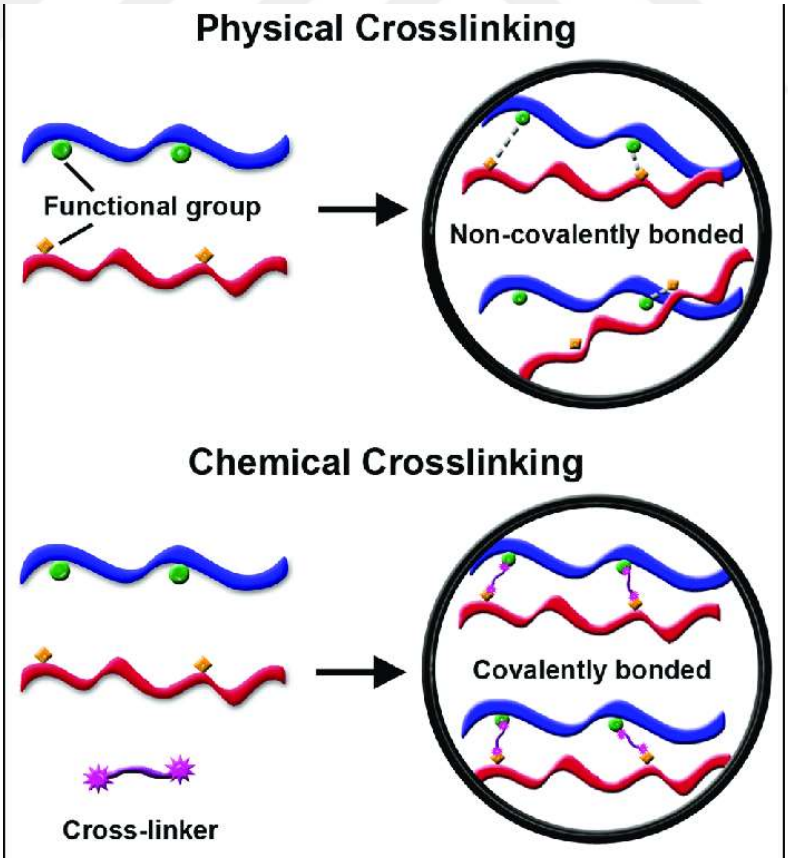

Figure 2.3 : Physical and chemical cross-linkings are graphically represented to demonstrate the type of bonding within the material [30].

Several strategies, such as double-network, nanocomposite, slide-ring, and macromolecular microsphere composite hydrogels have been created in recent years through the addition of sacrificial bonds to the hydrogel network that allow for major improvements in both the strength and elasticity of the system [31–34]. The distribution of strength under stress for such hydrogels was the key approach to obtaining mechanically strong hydrogels [35]. While chemically cross-linked hydrogels are brittle since there is an absence of energy dissipation under load, physically cross-linked ones are tough and dissipate energy.

2.2.1 Chemically cross-linked hydrogels

Covalent bonds connect the polymer chains in chemically crosslinked hydrogels. Chemically cross-linked gels have permanent junction points, therefore they are stable. They are also known as irreversible gels because they do not dissolve with changes in temperature, pH, or solvent composition. Generally, the formation of chemical gels was accomplished through the radiation-induced or chemical crosslinking of high molecular weight linear chains [36].

The fundamental disadvantage of chemically crosslinked hydrogels was their brittle nature limiting their application as load-bearing materials. Later, it was shown that the absence of effective energy dissipation was the reason for the mechanical weakness in their nature [10,37,38]. Chemically crosslinked hydrogels have low fracture energy because of fracture energy localization under deformation. When a high amount of chemical crosslinker is used, a rigid hydrogel network structure is obtained making the elastic character more dominant than viscous in the mechanical features of the gel. The viscous characteristic of the hydrogels contributes more to their mechanical features when the cross-linker amount is reduced. As illustrated in Figure 2.4, a low cross-link content in hydrogel leads to the production of a loosely connected network containing many entanglements able to create a high fracture energy, which is similar to the hydrogels containing physical interactions [39].

Deficiency of energy dissipation causes the fracture energy to be localized at the point of force application, resulting in rapid crack propagation and, as a result, fracture at low strain. Recently many studies have concentrated on formation of physical cross-linkings that effectively dissipate energy in hydrogels in order to avoid initiation and propagation of cracks when subjected to high deformation.

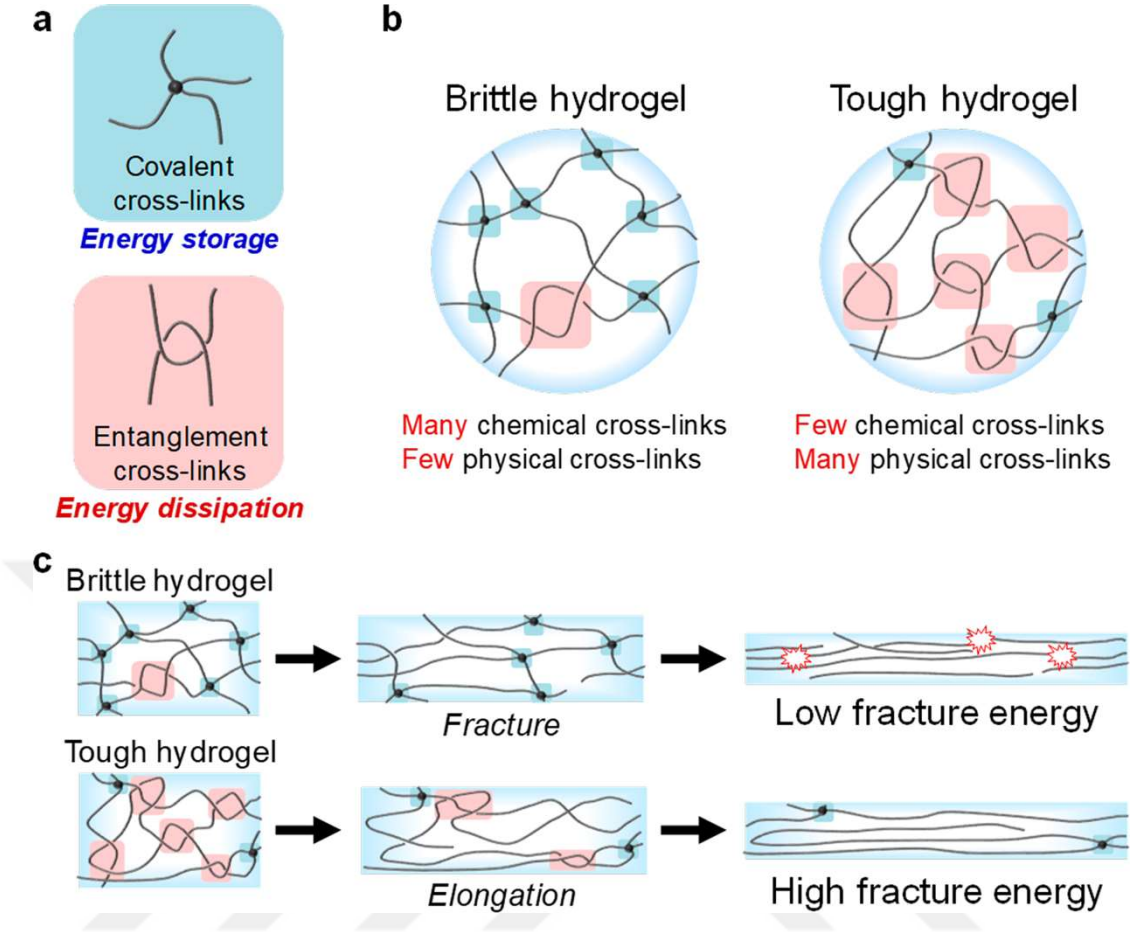

Figure 2.4 : (a) Covalent and entangled crosslinks are shown in the illustrations for energy storage and dissipation, respectively. (b) Structures of brittle and tough hydrogels that are chemically and physically crosslinked, respectively. (c) Brittle and tough hydrogel fracture behaviors with few and many entanglements, respectively [39].

2.2.2 Physically cross-linked hydrogels

Physically crosslinked hydrogels are formed as a result of cross-linking caused by physical interactions like ionic interaction, H-bond, coordination bond, and hydrophobic interaction. Because of the reversible nature of their cross-links, physical hydrogels generally exhibit reversible sol-to-gel transition and, they are also known as reversible gels. In hydrogels, there are several ways to create shape-memory and self-healing features by using reversible interactions. Moreover, due to their energy-dissipating gel network, mechanically strong and tough physically cross-linked hydrogels have been produced with dynamic properties.

2.2.2.1 H-bonding

H-bond is a weak interaction compared to covalent bonds and is formed by the attraction involving a hydrogen atom and a highly electronegative atom. H-bonds play a vital role in the development of supramolecular hydrogels and are essential for many biological and chemical systems. The characteristics of the atoms that create the hydrogen bonds, bond geometry, and the environment all have an impact on the bond strength. As a result, the selection of the quantity and type of H-bond-forming groups affects the mechanical characteristics of the gel.

Cooperative H-bondings between primary polymer chains are needed for the preparation of insoluble, water-stable, and mechanically strong physical hydrogels via H-bonds [18]. Exceptionally strong physical hydrogels via H-bonding have been created using H-bond acceptor and donor comonomers, dual amide groups, ureidopyrimidinone (UPy) units, and interactions between diaminotriazine and diaminotriazine (DAT-DAT). H-bonds linking polymer chains are quickly broken by water molecules because of their unstable behavior in an aqueous environment. As a result, H-bonds can be used to provide dynamic features for the targeted area due to their simplicity in breaking and reforming.

For example, it was reported that a PEG-cross-linked poly(2-vinyl-4,6-diamino-1,3,5-triazine) PEG-PVDT hydrogel exhibits ability to respond thymidine molecules for the regulated release of protein [40]. Figure 2.5 shows how the PEG-PVDT hydrogels react to thymidine. Thymidine-DAT has a significantly higher affinity than DAT-DAT. When the hydrogel comes into contact with thymidine the free thymidine molecules in solution flow into the hydrogel meshes and break the DAT-DAT H-bonding, and form thymidine-DAT H-bonding (Figure 2.5). DAT-DAT H-bonds regulate the total crosslinking density as well as the subsequent swelling ratio and in the proteins released from the hydrogel the presence of thymidine. According to the type and content of nucleoside, this particular nucleoside-sensitive feature may be used to regulate medication diffusion [41].

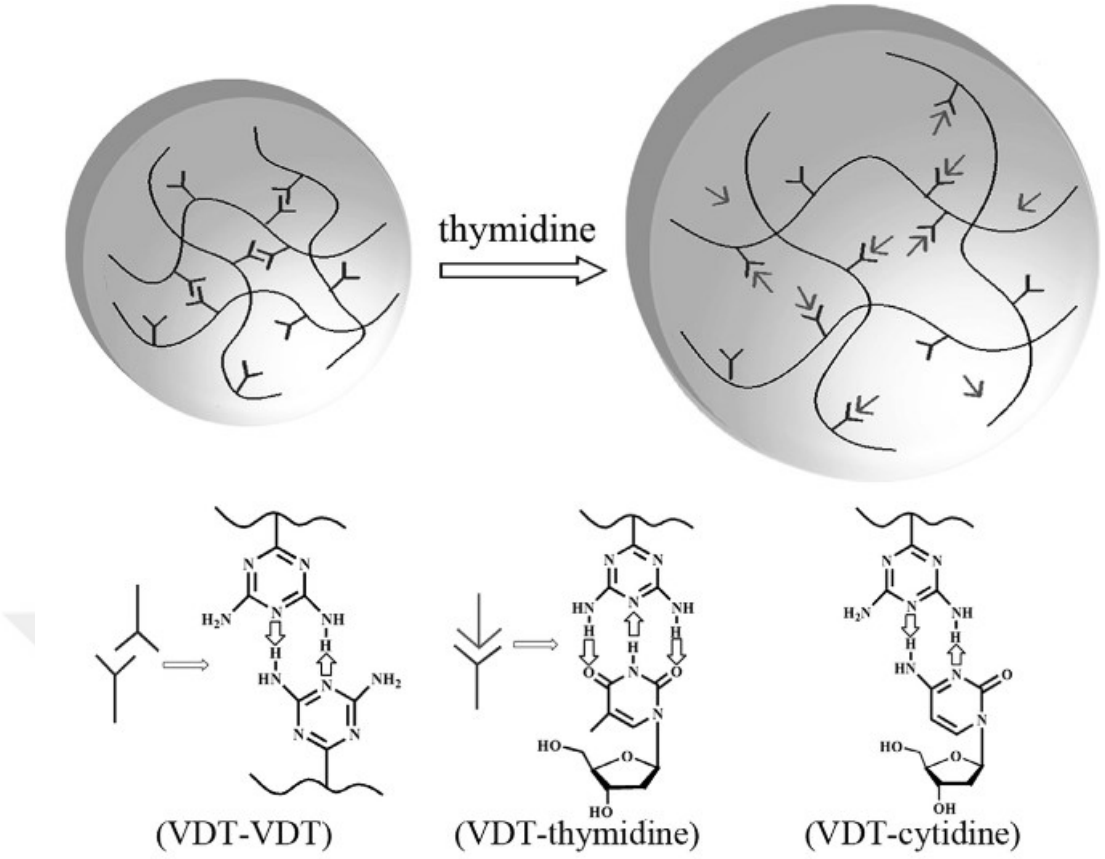

Figure 2.5 : Graphical representation of thymidine response mechanism of PEG-PVDT, and H-bonding of DAT residue groups with different guest molecules hydrogels are represented graphically [41].

Dimerization of ureidopyrimidinone (UPy) units forms complementary quadruple hydrogen bonding [42]. UPy units are attractive functionalities that can act as a bridge when they are introduced at chain terminals.

Supramolecules created by UPy units possess a variety of properties like strong mechanical strength, self-assembly, and self-healing, because of the large dimerization constant, selectivity, high strength, and reversibility of the H-bonds. In Figure 2.6 the synthesis procedure of at hydrogel consisting of N,N-dimethylacrylamide (DMAA), acrylic acid (AAc), and 2-(3-(6-methyl-4-oxo-1,4-dihydropyrimidin-2-yl) ureido) ethyl acrylate (UPyEA) units and, its strong and weak H-bonding interactions are shown. The hydrogel network formed of DMAA and AAc has a Young's modulus of 74±10 kPa, while incorporation of 0.2, 0.4, and 0.8 mol % UPy units increases the modulus to 283±18, 409±36, and 1,252±108 kPa, respectively. Tensile strain increased in response to an increase in UPy concentration. An increase in both modulus and tensile strain with increasing physical crosslink density is achieved through the

addition of UPy units to the network. This behavior was explained by the improved capacity of H-bonds to dissipate energy [43].

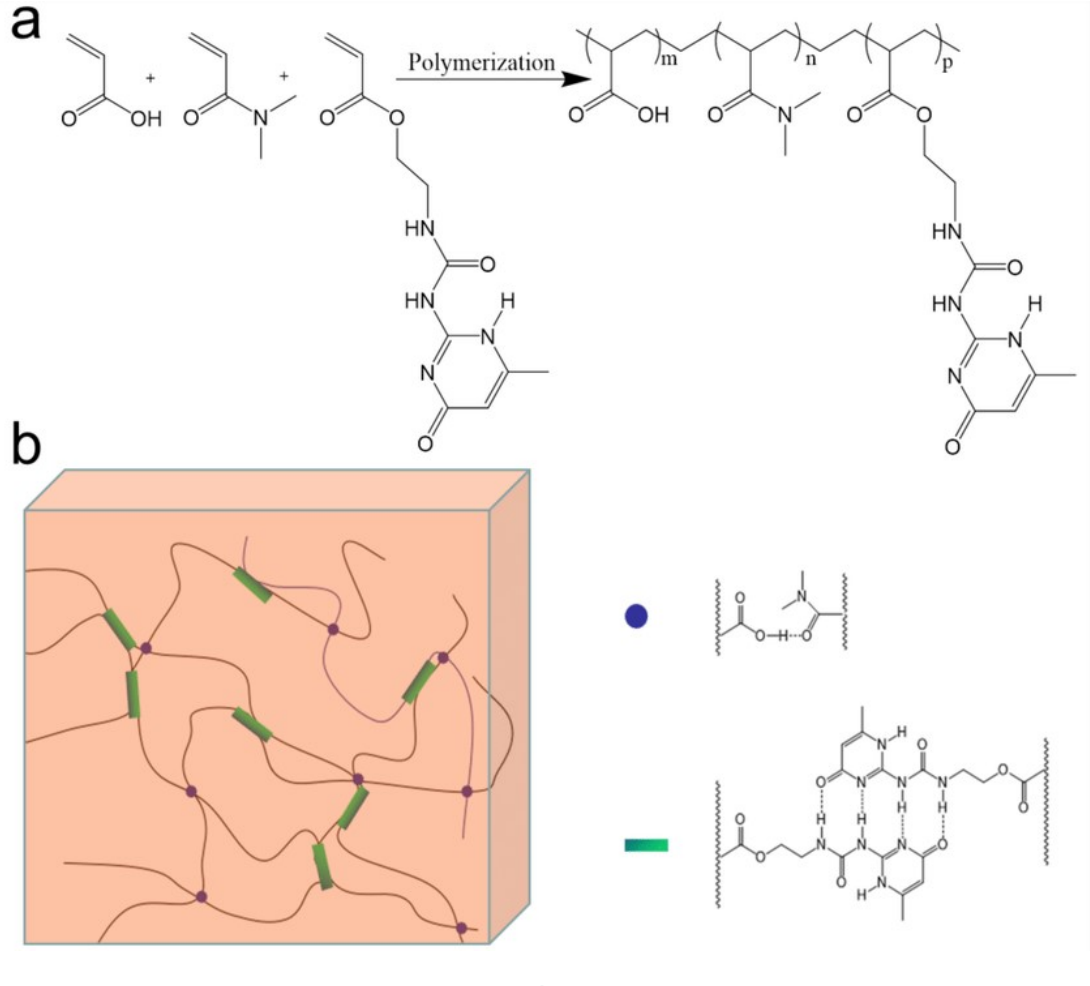

Figure 2.6 : (a) The polymerization reaction and the hydrogel structures. (b) Diagram exhibiting weak H-bonds linking acrylamides and acrylic acids, along with strong multiple H-bonds between UPy units [43].

Sheiko and colleagues have created poly(N,N-dimethylacrylamide-co-methacrylic acid) (P(DMAA-co-MAAc)) hydrogels with load bearing properties. In order to obtain tough hydrogels, H-bond was used as sacrificial bonds in a loose covalent hybrid network system. It was demonstrated that multiple H-bonds are formed between the carboxyl group of MAAc and the strong carbonyl group of DMAA, which results in the production of high amount polymer containing clusters that are supported through the hydrophobic associations of the MAAc α-methyl groups (Figure 2.7). These clusters serve as sacrificial cross-links to the hydrogel network, ensuring a high amount of energy dissipation. Although the free radical polymerization was conducted without any chemical crosslinker, it was confirmed that these hydrogels contain covalent cross-links, as demonstrated by their insolubility in aqueous solutions of urea

which is a well-known H-bond breaker. Covalent cross-linking was caused by the self-cross-linking of DMAA units. As a result, MAAc-co-DMAA networks can fully recover after deformation and display a high modulus of 28 MPa, and 800% elongation at fracture when incubated in an acidic environment. In contrast, the gel was extremely swollen and weak in pure water, with Young's modulus of 20 kPa, fracture stress, and strain of 17 kPa and 160%, respectively [44].

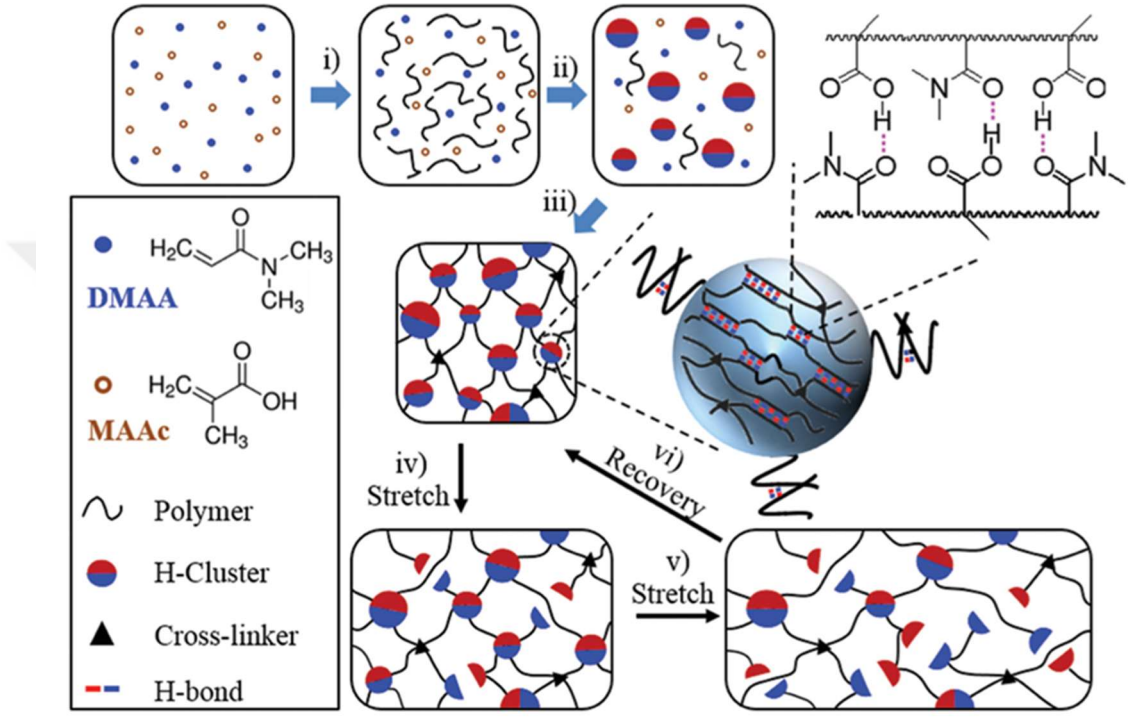

Figure 2.7 : Diagram illustrating the formation of P(DMAA-co-MAAc) hydrogels. i) Development of polymer chains; ii) Generation of polymer-rich clusters. iii The distance between adjacent clusters decreases, with increasing amount, density and overall dimensions of clusters. Subsequently, clusters are linked together by polymerization, which results in the production of macrogel. iv) Stretching the hydrogel results in the breaking of weak clusters; v) further stretching results in the fracture of strong clusters; vi) followed by overall recovery after unloading [44].

According to recent studies, hydrophobic domains have been proven to significantly increase the stability of hydrogen bonds in an aqueous environment. The hydrophobic groups efficiently induced the H-bond acceptor and donor groups to form stable hydrogen bonds [45].

As mentioned above, the dimer or multiple hydrogen-bonding units can affect the hydrogel characteristics such as mechanical strength, extensibility, and toughness. The density of H-bonds determined by the arrangement of H-bonding units further

influences the final properties of hydrogels. The number of multiple H-bonding units or the density of cross-linking have an important effect on the mechanical performances of the hydrogels.

2.2.2.2 Ionic interactions

The electrostatic attraction of oppositely charged ions/groups causes ionic interactions. Interaction between an ion and a dipole (polar group) can lead a non-polar molecule to polarize (induced dipole). The attraction of anionic functionalities like carboxylates, sulfates of polymers, to cationic groups like protonated amines, also oppositely charged ions and other charged functional groups of polymers can result in the production of hydrogels. The creation and stability of these hydrogels are influenced by the ionization degree of their charged groups, ionic strength, pH, concentration, and temperature.

Polyelectrolyte hydrogels that contain both cationic and anionic groups are called polyampholytes. Depending on how permanent each form of charge is, hydrogel formation results in four options; (i) Both weak anionic and cationic groups; (ii) Both strong anionic and cationic groups; (iii) Strong anionic and weak cationic groups; (iv) Weak anionic and strong cationic groups. These are frequently used options to categorize the strengths and charges of these functionalities. Polyampholytes have an adjustable isoelectric point that is determined by the choice of the underlying functionalities. When a polyampholyte has an overall neutral charge, the isoelectric point occurs at that pH level [46,47].

Though polyampholyte hydrogels exhibiting properties such as self-healing, toughness, and salt-responsiveness were first synthesized by Gong et al. in the absence of chemical cross-linker [48,49]. They were obtained easily by a one-step mixing procedure by carrying out random polymerization of counter-charged monomer units in the salt solution near the charge balance. The presence of net charges on the polymer chains gives rise to the high water swelling of weak electrolyte polyampholyte hydrogel which is, in contrast to conventional polyampholyte hydrogels made of strong electrolytes [50,51]. As can be seen from Figure 2.8 these hydrogels contain strong and weak bonds acting as primary and sacrificial bonds, respectively. Since the strong connections work as primary crosslinks, the weak bonds, which form

recoverable sacrificial bonds and rapidly break under deformation, release energy to inhibit crack development [48].

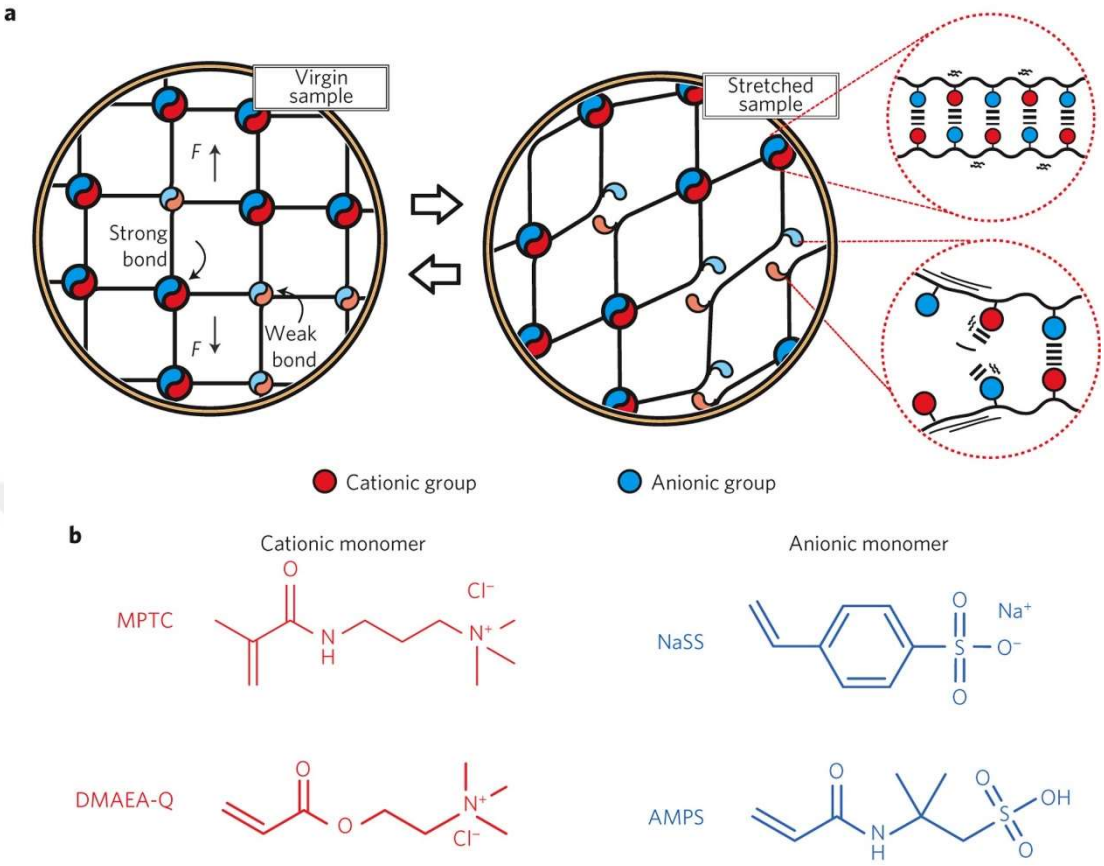

Figure 2.8 : (a) A demonstration of polyampholyte networks with variable strong ionic interactions. The strong bonds work as permanent cross-linking points, whereas the weak bonds serve as reversible sacrificial bonds that fracture under load. (b), The chemical structures of monomers employed in this study. MPTC and DMAEA-Q are cationic monomers, while NaSS and AMPS are anionic monomers [48].

2.2.2.3 Hydrophobic interactions

In structural biology, hydrophobic interactions are essential like H-bonds for instance in proteins. The core of the proteins is the place where non-polar particles are present and responsible for the hydrophobic forces. They can also be used to develop supramolecular hydrogels. Compared to H-bonds and van der Waals interactions, hydrophobic associations are stronger. The production of gels through hydrophobic interactions are possible to generate by using molecules containing both hydrophilic and hydrophobic parts. To reduce their contact with water, the nonpolar moieties develop hydrophobic interactions with one another. As a consequence, the core-shell structure forms and hydrophobic domains lie in the center of the folded amphiphilic chains in water, which are encircled by polar groups that are subjected to the aqueous

environment. The molecules aggregate, combine, and eventually form micelles, resulting in the formation of the entire gel, when the minimum gelling concentration is attained. To create an energy-dissipating, tough hydrogel network, our research group has modified hydrophilic polymer chains with hydrophobic long alkyl side chains by using the micellar polymerization technique [9,52–64]. This simple strategy uses free radical polymerization to graft the hydrophobic side chain onto the hydrophilic chain. Copolymerization of the hydrophobic monomer with the hydrophilic monomer takes place in the aqueous solution after being solubilized inside the micelles. Due to the high localized concentration of hydrophobes inside the micelles, the hydrophobic monomers are randomly dispersed as blocks throughout the hydrophobic polymer main chain.

Figure 2.9 : The images of two hydrophobically modified hydrogel specimens prepared in 0.5 M NaCl are shown. One of them was colored for clarity. After being divided into two halves, then brought together at the cut surfaces, the specimens rejoint into a single piece [53].

Using this technique, large hydrophobes such as stearyl methacrylate (C17.3) consisting of 65% n-octadecyl methacrylate and 35% n-hexadecyl methacrylate, and dococyl acrylate (C22) were copolymerized with acrylamide without any chemical cross-linker in a micellar system modified by salt addition. The addition of a sufficient amount of an electrolyte such as NaCl weakens electrostatic interaction leading to spherical SDS micelles growing bigger and solubilization of large hydrophobic monomers within the grown micelles. In order to compare their properties, traditional chemically cross-linked PAAm gel and PAAm gel containing both chemical cross-linker and C17.3 hydrophobic associations were also synthesized alongside with PAAm gel containing only the hydrophobic associations of C17.3 units. The results highlight the exceptional mechanical performance of the hydrophobically modified physical hydrogels, especially given that the chemical PAAm hydrogels made under identical experimental circumstances rupture at only a few ten percent elongation. The produced hydrogels have a high level of toughness and self-healing effectiveness due to the dynamic character of the merging zones linking the network chains, which are

strong hydrophobic associations between the C17.3 blocks that inhibit dissolution in water and flow (Figure 2.9) [53].

Another study from our research group focused on the hydrophobically modified polyampholyte hydrogels prepared by micellar polymerization using equimolar amounts of 2-acrylamido-2-methylpropane-1-sulfonic acid sodium salt (AMPS) and (3-Acrylamidopropyl)trimethylammonium chloride (APTAC) monomers in the existance of the varying amounts of the hydrophobic monomer octadecyl acrylate (C18A). Chemically cross-linked polyampholyte hydrogels were created at different AMPS mole fractions in the first part of the study to emphasize the exceptional qualities of the hydrophobically modified physical polyampholyte hydrogel. Mechanical tests showed that hydrophobically modified hydrogels were stiffer than the chemically cross-linked ones and their water-swollen state showed better mechanical performance than their as-prepared state. Furthermore, cut-heal ability was confirmed at 50 °C revealing that they can be healed after which they fully recover their original Young's modulus after 1-4 hours of waiting time [65].

2.2.2.4 Coordination bond

In order to form self-healing hydrogels, metal coordination bonds are frequently utilized as dynamic crosslinkers. Researchers have been motivated to discover new approaches to develop advanced materials as a result of a better understanding of the underwater attachment mechanism used by mussels and other marine animals. Materials were created functionalized with 3,4-dihydroxyphenylalanine (DOPA), a catecholic amino acid, and its analogues for moisture-resistant coatings, adhesives, and especially supramolecular hydrogels based on ligand-metal coordination bonds [66–72]. As stretchability and self-healing are all closely tied to the adaptable properties of the identical metal coordination links, it is still difficult to individually increase the toughness of metal-coordinated hydrogels without also altering these aspects [73].

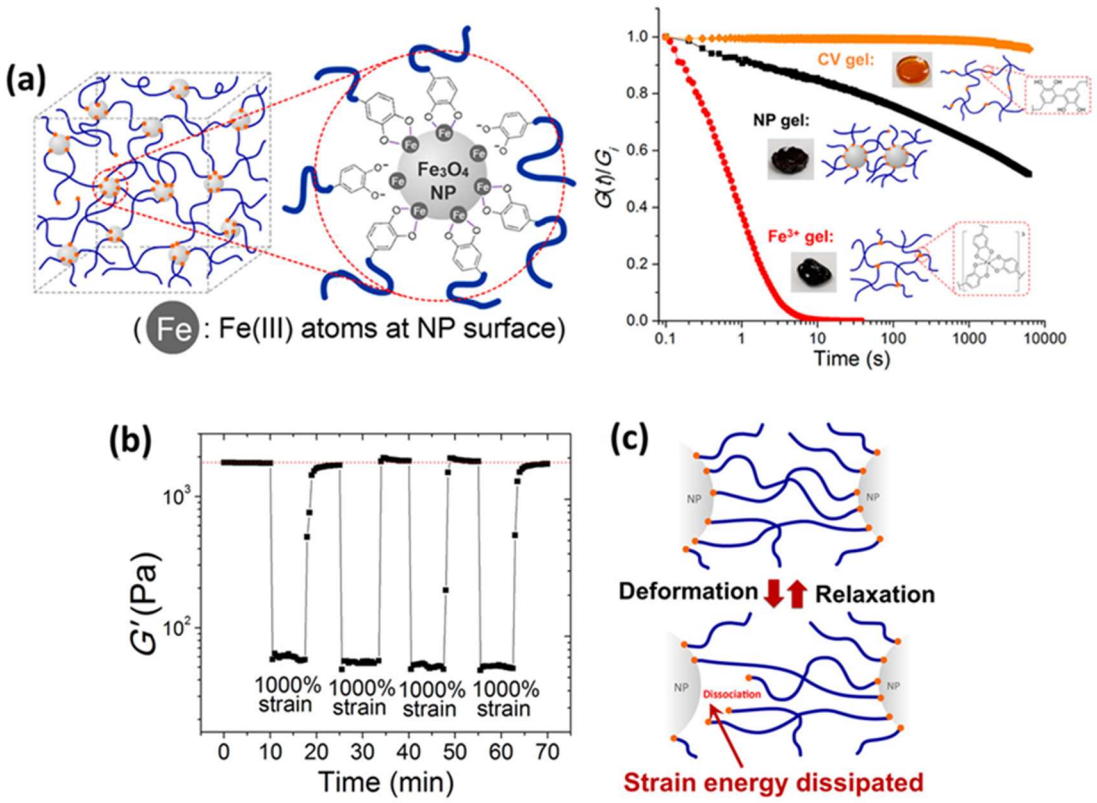

Figure 2.10 : (a) Schematic illustration of Fe_3O_4 nanoparticle-crosslinked hydrogel (NP gel) and step strain (10%) relaxation curves of NP, Fe^{3+}, and CV gels at 20 °C. The recorded initial relaxation modulus G_i is used to normalize $G(t)$. (b) Strain amplitude step test of NP gels interchanging between 1% and 1000% oscillatory shear strain ($\omega = 1$ rad s^{-1}). (c) Diagram showing the reversible association-dissociation of catechol functionalities at NP surfaces that dissipate deformation energy in NP gel [72].

Due to the cooperative breaking of these bonds during stress, increasing the coordination number has a positive impact on the mechanical performance of the gels [74]. In order to develop hydrogels that are crosslinked using reversible metal-coordination connections at Fe3O4 NP surfaces, Holten-Andersen et al. have added iron oxide nanoparticles (Fe3O4 NPs) to a catechol-functionalized polymeric gel network. They were developed by the inspiration of adhesive chemistry in mussels. The hydrogels became significantly tougher while remaining reversible by increasing the number of crosslinking sites utilizing Fe_3O_4 nanoparticles rather than Fe^{3+} ions with catechol. The findings provide quantitative information about three types of hydrogel networks and their impact on mechanical properties. Permanent covalent inter-catechol cross-links (CV gel) in the gel network prevent them from relaxing and reorganizing to release strain energy (Figure 2.10a). The stress is reduced by both the NP and Fe^{3+} gels when their reversible coordination cross-links can dissociate and

reassemble to form a new network. (Figure 2.10b, c). At the polymer-nanoparticle interface in the hydrogel network, the resultant hydrogel dynamics are in direct coupling with the reversible coordinate crosslink mechanics. The reversibility and dynamic properties are obtained by forming a metal coordination bond between polymer and nanoparticle [72].

2.2.2.5 *π-π* stacking

Interactions between aromatic rings with π orbitals are referred to as π - π stacking interactions, and they could be extremely important in a variety of chemical applications. It is common knowledge that π - π interactions are crucial for the thermal stability and folding of proteins. A structural foundation for π - π interactions is provided by the aromatic group in the phenylalanine residue of proteins and the base residue of nucleic acids. Anticancer drug delivery systems based on π - π interaction with self-assembled DNA nanotubes have been investigated [75]. Additionally, researchers have been looking at using carbon nanotubes and nanomaterials based on graphane to transport drugs, nucleic acids, and proteins by π-π interactions [76–78]. Multilayer graphene, single-layer graphene, graphene oxide (GO), and reduced graphene oxide (rGO) are all graphene-based nanomaterials and they have a honeycomb lattice structure [77]. Every carbon atom in graphene-based nanomaterials has π electrons in a honeycomb lattice structure [79].

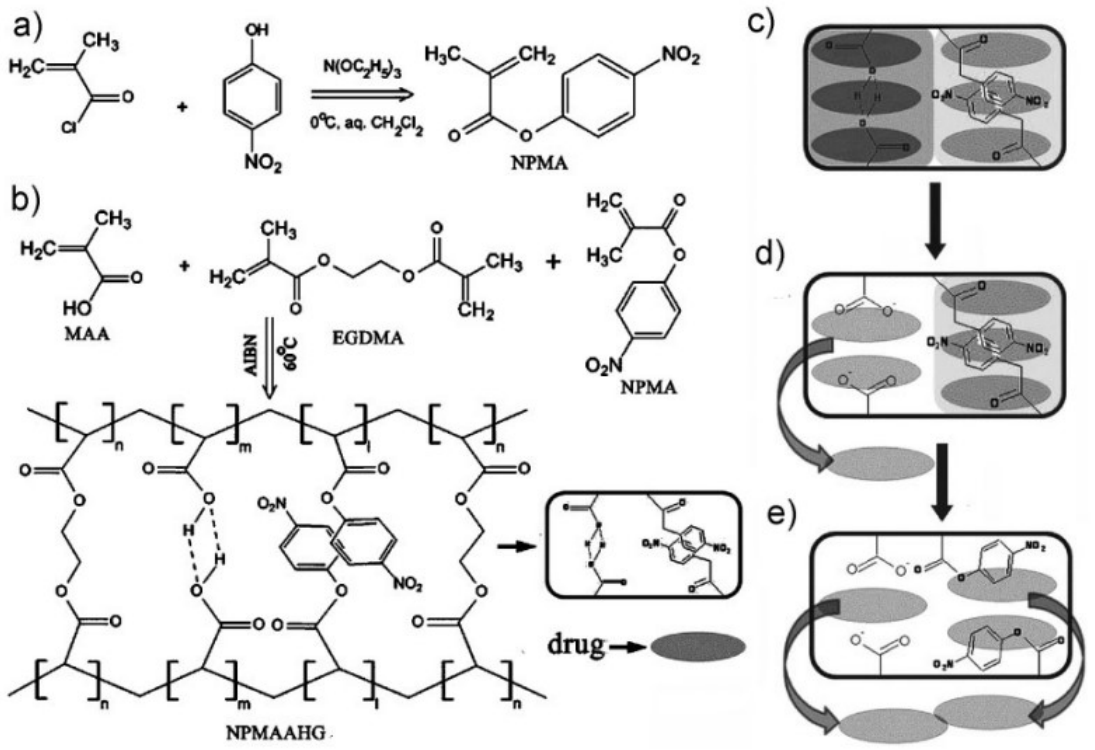

Figure 2.11 : Schematic depiction of the structure, production, and co-switched medication release mechanism of the NPMAAHG hydrogels. (a) Preparation of the functional comonomer NPMA. (b) NPMAAHG hydrogel preparation by the copolymerization of NPMA with MAAc and using EGDMA as a crosslinker. The π - π stacking and H-bonding interactions that are formed by the carboxylic acid groups and NPMA segments, respectively, serve as switches to regulate the release of guest molecules. (c) At low pH (1.4), drugs are closed in NPMAAHG; π - π stacking and H-bonding interactions operate as off-status switches to delay the release of drugs. (d) Due to the H-bond switch being opened in basic solution, drugs only partially release from the NPMAAHG networks; the π - π stacking switch is still present. (e) Drugs release further because of the swelling of hydrogels opening the π - π stacking switch [80].

The creation of hydrogels for controlled drug release has been made possible via π - π stacking and H-bonding interactions. A poly(nitrophenyl methacrylate-co-methacrylic acid) (NPMAAHG) gel was prepared by copolymerization of functionalized 4-nitrophenyl metacrylate (NPMA) and methacrylic acid (MAAc) monomers and 4-nitrophenyl methacrylate segments with glychol dimethacrylate (EGDMA) crosslinker. Hydrophobic properties of π - π stacking can offer a hydrophobic region to hold hydrophobic drug molecules. The carboxylic acid groups and 4-nitro methacrylate segments in hydrogel form H-bond and π - π stacking, respectively, that function as switches to regulate the release of molecules by varying the ratio of these interactions (Figure 2.11c). As a result, kinetics of drug release behavior and properties

like high pH sensitivity, and excellent swelling were investigated for this hydrogel. pH-sensitive drug release mechanism of the hydrogel can be seen in Figure 2.11(c-e). At high pH (7.4), drugs are partially released because H-bonds are canceled due to the ionization of carboxylic acid groups, leaving the network under the influence of π – π stacking (Figure 2.11d). As the hydrogels swell, π – π stacking associations slowly become weaker and drug molecules are further released (Figure 2.11e). At low pH (1.4), both π - π stacking and H-bonding interactions act as physical cross-linking to maintain drug molecules inside of the structure (Figure 2.11c) [80].

2.2.2.6 Host-guest interactions

Another way to create physical hydrogels is forming cross-links via host-guest supramolecular complexation. One macrocyclic host molecule containing a cavity can engage with one guest molecule by physical interactions. In supramolecular chemistry, cyclodextrins (CD) as naturally derived host have received the majority of attention. CD consists of an exterior hydrophilic surface and a hydrophobic cavity [81]. The three most common cyclodextrin forms are designated as α-CD, β-CD, and γ-CD and contain six, seven, and eight d-glucose units, respectively. α-CD interacts physically with linear guests because of its small cavity size, whereas β-CD can host polymer chains as well as larger, more spherical guests like adamantane or azobenzene [82,83].

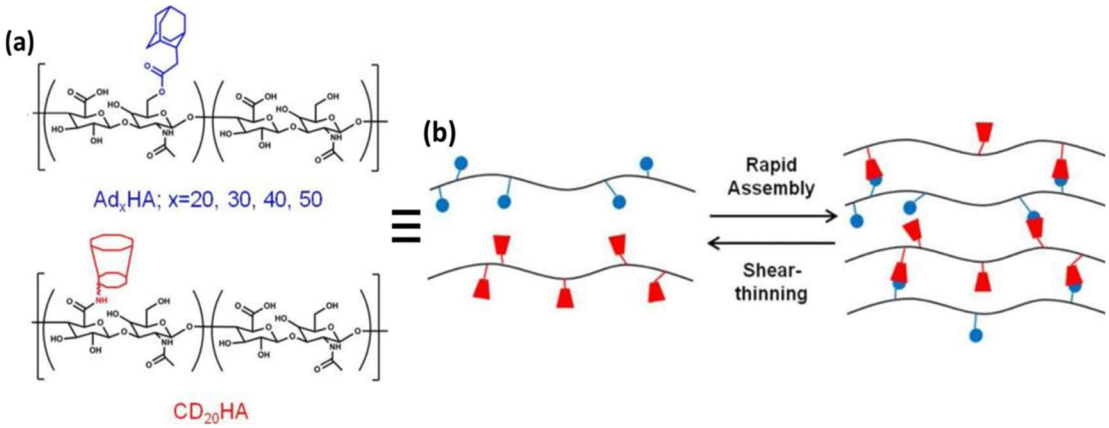

Figure 2.12 : Mechanism of hydrogel production. (a) Chemical structures of adamantane-modified hyaluronic acid (Ad-HA) and β-CD-modified hyaluronic acid (β-CD-HA) (b) Diagram illustrates the development of dynamic cross-links using guest-host complexation [82].

For instance, hyaluronic acid (HA) was individually modified by host β-cyclodextrin and guest adamantane (Ad). The produced host and guest macro monomers were both

found to be viscous solutions, and oscillatory rheology demonstrated that mixing led to an increase in modulus of several orders of magnitude. It was shown that the two macromer components could be simply mixed to form a hydrogel. As can be seen from Figure 2.7 the guest-host interactions between Ad and β-CD functionalities as physical cross-links. To arrange cross-linking density, the concentrations of Ad-HA and β-CD-HA macro monomers or the molar fraction between Ad and β-CD units are utilized to regulate the cross-linking density. The flow and recovery characteristics of the resulting gels were investigated and found as capable of shear-thinning behavior for biomedical applications [82].

2.3 Superabsorbent Hydrogels

When compared to other absorbent materials, superabsorbent hydrogels are three-dimensional lightly cross-linked hydrophilic polymers that have the capacity to hold a high amount of water. In their dry condition, macromolecular chains that form hydrogel networks acquire coil conformation, but when exposed to water or an aqueous media, they considerably expand their structure to an immense size [84]. As a result, these water molecules are retained inside the 3D network (Figure 2.13).

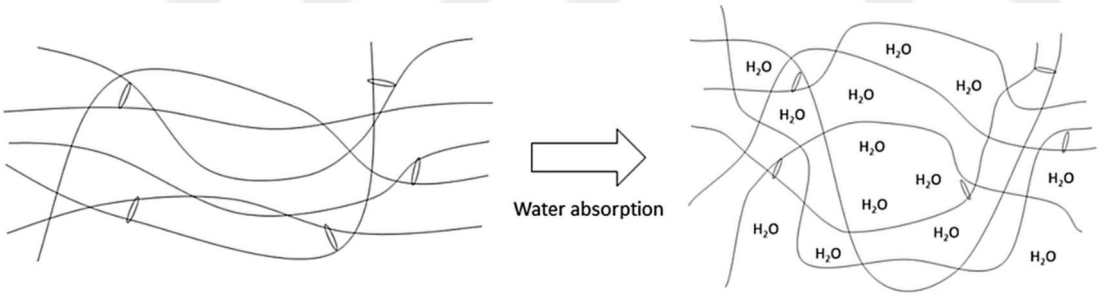

Figure 2.13 : A superabsorbent polymer network is shown schematically with cross-linking agents (ellipses) before and after swelling as a result of water absorption [85].

The most extensively investigated and produced superabsorbent polymers (SAPs) are hydrogels based on derivatives of acrylic acid [86,87]. Lightly cross-linked poly(acrylic acid) (PAAc)-based hydrogels are used in hygiene products like napkins, and diapers. Unfortunately, the original PAAc-based SAPs are mechanically weak and quickly swell due to their loosely cross-linked structure [88].

Although a strongly cross-linked hydrogel system can preserve its integrity when it is swollen. It exhibits a low degree of swelling because of the high crosslinking density. That is due to the short chain length between its network junctions limiting the water

absorption and hence leading to a low swelling degree. A careful balance must be maintained between elastic and swelling forces in hydrogel swelling. A hydrogel with hydrophilic ions and functional groups can produce intense contact with the surrounding solution, which leads to hydrogel expansion. Conversely, cross-links stop an infinite network from growing by creating elastic forces. The ionic strength and pH of the solution have an important influence on the swelling capacity of many hydrogels. The elastic effect produces a force that causes the 3D network to shrink before achieving equilibrium with a force that causes the network to expand through swelling. The osmotic pressure caused by the concentration differences in the external and internal medium of the hydrogel of mobile ions determines this absorbing force. The amount of swelling is affected by the cross-linked density, as well as the quantity of immobilized polarizable functional groups on the polymer backbone [84].

2.4 AMPS-Based Hydrogels

2-acrylamido-2-methyl-1- propanesulfonic acid (AMPS) is a polyelectrolyte monomer that can be used to obtain hydrogels with a high level of water swelling capacity. Thousands of patents and papers now address the use of this monomer in various industrial applications, in contrast to the 1970s when it was exclusively used to make acrylic fiber [89]. The hydrophilic character, thermal consistency, preserving its structural integrity across a broad pH range, and ionic character of the polymer are all improved by AMPS. Since an aqueous solution was used to carry out the polymerization, water is held within a three-dimensional cross-linked structure. As a result, an already hydrated hydrogel is produced and this synthetic hydrogel has the advantages such as softness and flexibility.

2.4.1 Chemically cross-linked AMPS-based hydrogels

AMPS has captured interest because of its highly ionizable sulfonate group, which dissociates entirely in the entire pH range. Thus, chemically cross-linked hydrogels composed of AMPS have excellent electro-responsiveness and swelling behavior that is independent of pH. Moreover, different monomers were copolymerized with AMPS in the existence of chemical cross-linkers to generate hydrogels with tunable swelling ratios. Since poly(AMPS) (PAMPS) hydrogels, are typically prepared by chemical

crosslinks, they show poor mechanical behavior which restricts their potential applications [6–8].

AMPS hydrogels that are chemically crosslinked with N,N'-methylene-bis-acrylamide (MBA), or glycol dimethacrylate (EGDM) were produced by Nalampang et al. with the purpose of biomedical use as wound dressing materials. Hydrogel preparations were conducted at room temperature by redox initiating system at different monomer concentrations and initiator contents. They showed that hydrogels produced at the monomer concentrations of between 40-60% w/v can be cast into good-quality sheets with the right amount of flexibility and water absorption, making them ideal for wound dressing applications. However, the rubbe highly influences the swelling of the hydrogels by increasing the resistance to matrix expansion. When higher percentages of crosslinker (0.5-1.5 mol %) were used, more compact 3-dimensional hydrogel structures formed [90].

2.4.2 Physically cross-linked AMPS-based hydrogels

Xing et al. were made a pioneering study to create physical PAMPS hydrogels without the use of chemical crosslinkers and initiators by utilizing thermal polymerization of AMPS-containing water solutions at 80 °C [91]. However, the strength of the H-bonds linking the amino and carbonyl functionalities of the AMPS units was not enough to survive the osmotic pressure of AMPS counterions, causing the hydrogels to dissolve readily in water despite having self-healing effectiveness and a high stretchability (2,500%) [91–93]. As can be seen from Figure 2.10b, after being cut into two and rejoint together for 30 min, the PAMPS specimen containing 20 wt% water can self-heal without any external trigger. The healed sample can carry 1.5 kg weight. Multiple dynamic inter-chain H-bonds forming between the cut surfaces of the PAMPS sample is the reason of an impressive rate of self-healing. Water content is an important parameter for mechanical properties as well as healing time. As seen in Figure 2.10c, PAMPS hydrogel containing 47 wt% of water can self-heal after 10 days in a closed environment and its break strength is about 1000 times lower than that of 20 wt% water containing PAMPS hydrogel. Therefore, increasing total monomer concentration and H-bonding cooperativity can be a good strategy to improve mechanical features and self-healing effectiveness [91].

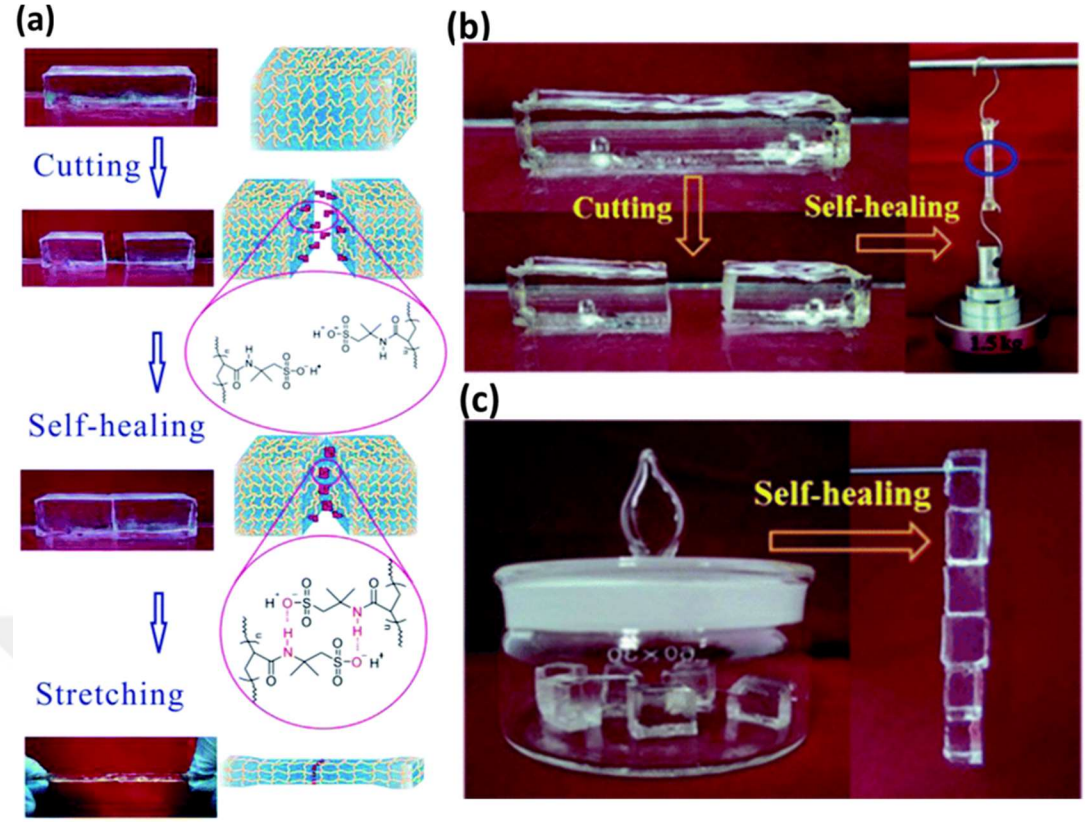

Figure 2.14 : (a) Visualisation of the self-healing process and mechanism. (b) After being cut into two pieces, the PAMPS sample containing 20 wt% water can instantly self-heal. The healed sample can support a 1.5 kg weight without suffering any noticeable damage. (c) After storing the PAMPS hydrogel containing 47 wt% water in a sealed weighing vial for 10 days, the sample can self-heal naturally without any external stimuli [91].

2.4.3 Superabsorbent AMPS-based hydrogels

A recent study from our research group showed that UV polymerization of AMPS without the use of chemical cross-linking agent results in the production of water-insoluble PAMPS hydrogels with a swelling ratio of about 1000 g/g (Figure 2.15). In the last few years, researchers have been focusing on PAMPS hydrogels, enhancing their mechanical performance, and creating self-healing behavior. In the same study, in the absence of a chemical crosslinker, copolymerization of AMPS and DMAA boosts the H-bonding cooperativity and produces exceptionally strong physical hydrogels. AMPS/DMAA hydrogels have a high Young's modulus (up to 0.41 MPa), tensile strength (~0.57 MPa), and fracture strain (~1,000%) in their as-prepared state. In this study, the properties that make these hydrogels special are high water absorbance capacity (up to 1,700 g/g) with the ability to maintain its shape at swelling

equilibrium, complete self-healing efficiency without any treatment, and as previously mentioned improved mechanical properties by using H-bonds [18].

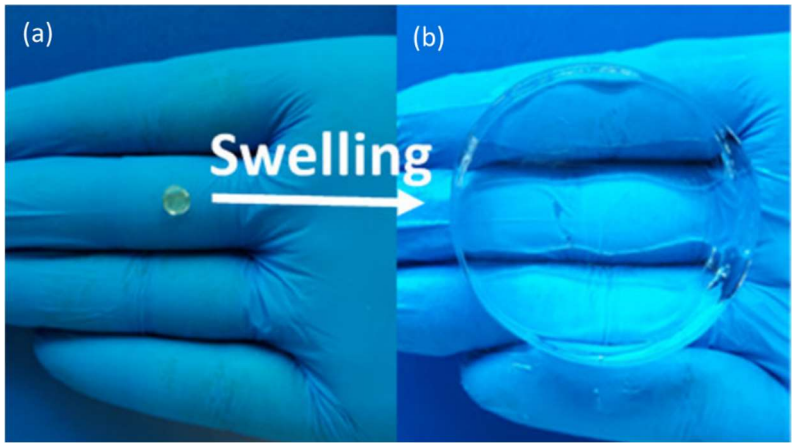

Figure 2.15 : Images of a UV polymerized AMPS/DMAA hydrogel specimen prepared at the monomer concentration of 60 wt% (a) as-prepared and (b) after equilibrium swelling in water [18].

3. EXPERIMENTAL PART

3.1 Materials

2-Acrylamido-2-methylpropane-1-sulfonic acid (AMPS, 99%, Sigma-Aldrich), Methacrylic acid (MAAc, 99%, Merck), N,N- dimethylacrylamide (DMAA, 99%, Sigma-Aldrich), 2-hydroxy-4′-(2-hydroxyethoxy)-2-methylpropiophenone (Irgacure 2959, 98%, Sigma-Aldrich), and poly(ethylene glycol) (PEG, 10000 g·mol^{-1}, Sigma-Aldrich) were used as received. Acrylic acid (AAc, 99%, Merck) was used after inhibitor removal by passing through a column filled with inhibitor remover (Sigma-Aldrich). The chemical structures of the monomers are given in Figure 3.1.

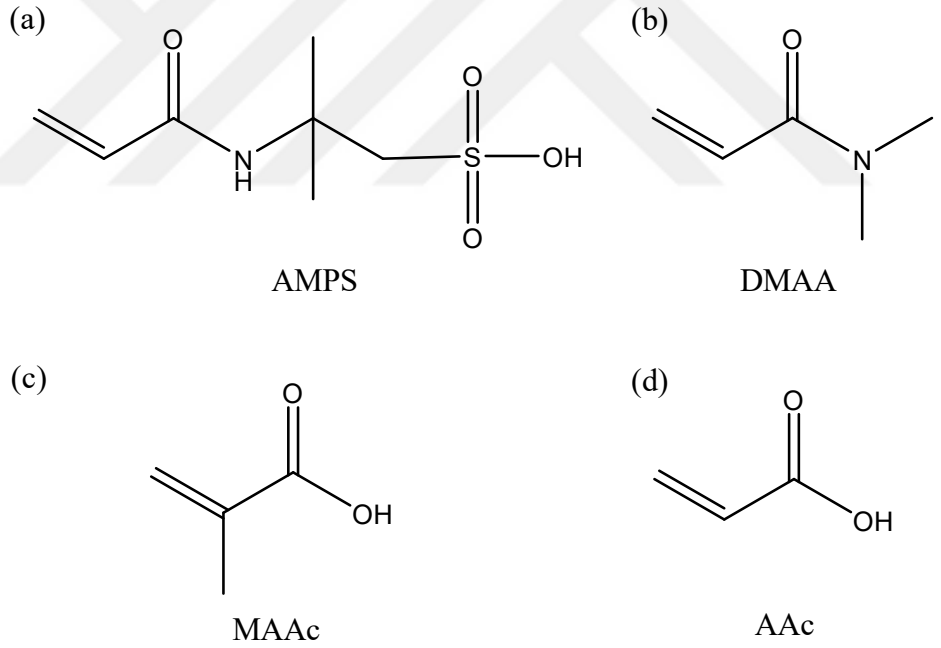

Figure 3.1 : The chemical structures of monomers: (a) 2-Acrylamido-2-methylpropane-1-sulfonic acid (AMPS), (b) N,N- dimethylacrylamide (DMAA), (c) methacrylic acid (MAAc), and acrylic acid (AAc).

3.2 Preparation of Hydrogels

There are mainly three experimental parameters, namely the water content *w*, the mole fraction x_{co} of the comonomers MAAc and DMAA, and the molar fraction x_{MAAc} of MAAc in the MAAc+DMAA mixture which are calculated by,

$$w = 1 - \frac{mass\ of\ AMPS + MAAc + DMAA}{mass\ of\ the\ solution} \tag{3.1}$$

$$x_{co} = \frac{moles\ of\ MAAc + DMAA}{moles\ of\ MAAc + DMAA + AMPS} \tag{3.2}$$

$$x_{MAAc} = \frac{moles\ of\ MAAc}{moles\ of\ MAAc + DMAA} \tag{3.3}$$

The preparation of hydrogels involved the UV-polymerization of AMPS aqueous solutions containing the comonomers DMAA, AAc, MAAc, and Irgacure 2959 photoinitiator in the absence of chemical crosslinker at 23±2 °C. In our experiments, a fixed amount of AMPS (0.012 mol) was used at a comonomer mol ratio (x_{co}) of 0.62 to compare the results with those of AMPS/DMAA ones reported before [18]. The amount of Irgacure 2959 was 0.2 mol% with respect to the total monomer content.

The first set of hydrogels were produced by copolymerization of AMPS with DMAA, MAAc, and AAc at a constant water content *w* of 25 wt% as detailed in Table 3.1.

Table 3.1 : Comonomer effect (*w* = 25 wt%).

Comonomer type	AMPS / g	Comonomer / g	Deionized water/ g	Irgacure/ mg
DMAA	2.5	2.0	1.5	15
MAAc	2.5	1.7	1.4	15
AAc	2.5	1.4	1.3	15

Then, AMPS/MAAc/DMAA terpolymer hydrogels were generated at various molar fractions of MAAc in MAAc + DMAA comonomer mixture, denoted as x_{MAAc} (Table 3.2).

Table 3.2 : Effect of x_{MAAc} (w = 25 wt%).

x_{MAAc}	AMPS / g	MAAc / g	DMAA / g	Deionized water / g
1.0	2.5	1.7	-	1.4
0.8	2.5	1.4	0.4	1.4
0.7	2.5	1.2	0.6	1.4
0.6	2.5	1.0	0.8	1.4
0.5	2.5	0.9	1.0	1.4
0.4	2.5	0.7	1.2	1.5
0.2	2.5	0.3	1.4	1.5
0.0	2.5	-	2.0	1.5

At last, the water content (w) was varied from 25 to 99 wt% at a fixed MAAc mol fraction (x_{MAAc} = 0.8), as indicated in Table 3.3.

Table 3.3 : Effect of water content (x_{MAAc}= 0.8).

***w* wt%**	**AMPS / g**	**MAAc / g**	**DMAA / g**	**Deionized water / g**
25	2.5	1.4	0.4	1.4
30	2.5	1.4	0.4	1.8
40	2.5	1.4	0.4	2.9
50	2.5	1.4	0.4	4.3
75	2.5	1.4	0.4	12.8
80	2.5	1.4	0.4	17.2
90	2.5	1.4	0.4	38.7
95	2.5	1.4	0.4	81.7
99	2.5	1.4	0.4	425.7

The synthesis procedure for the synthesis of terpolymer hydrogel at w = 25 wt%, x_{co} = 0.62, and x_{MAAc} = 0.8 follows: A certain amount of AMPS (2.50 g, 0.012 mol) was first dissolved in deionized water (1.4 g). Comonomers MAAc (1.40 g, 0.016 mol) and

DMAA (0.40 g, 0.004 mol) were the added to this aqueous solution. After 10 min of stirring and nitrogen N_2 bubbling, Irgacure 2959 initiator (14.4 mg, 0.2 mol % of the monomers) was added and mixed. The solution was drawn into 1 mL disposable plastic syringes of 4.6 mm internal diameter and polymerization was conducted at 23±2 °C for 24 hours in an UV reactor at a wavelength of 360 nm.

3.3 Swelling Tests and Gel Fractions

The hydrogels synthesized in the syringes were sliced into specimens that were about 2 mm long, and they were then submerged in an abundance of deionized water at 23 °C for 10 days, changing the water periodically to remove any soluble polymers, unreacted monomers, and the initiator. Once the swelling equilibrium was reached, the swollen hydrogels were removed from the water and freeze-dried (Christ Alpha 2e4 LD-plus). Dried polymer was weighed and the gel fraction W_g was determined by equation (3.4),

$$W_g = m_{dry} / (m_o C_o) \tag{3.4}$$

Where C_o (1-w) is the total monomer concentration of the hydrogel, the mass of the specimen just after synthesis is referred as m_o and after drying the swollen gels, the mass is referred as m_{dry}. The relative weight swelling ratio m_{rel} was determined by equation (3.5),

$$m_{rel} = m / m_o \tag{3.5}$$

where mass of the equilibrium swollen gel sample is referred as m.

Furthermore, for copolymer hydrogels, swelling tests with various pH values were conducted for 10 days by replacing medium everyday. All hydrogels had their swelling measurements repeated at pH levels varied between 2 and 10. pH values of aqueous solutions were arranged by using NaOH and HCl solutions.

4. CHARACTERIZATION PART

4.1 Elemental Analysis

Elemental analyses were performed on freeze-dried specimens using a CHNS-932 (LECO) elemental analyzer.

4.2 Fouirer Transform Infrared Spectroscopy (FTIR) Analyzes

Fourier-transform infrared (FTIR) spectroscopy was performed on an Agilent Technologies Cary 630 FTIR instrument with an Attenuated Total Reflection (ATR) module in the wavelength interval range of 4000–400 cm^{-1}.

4.3 Scanning Electron Microscopy (SEM)

The morphologies of hydrogels at various water contents were examined using scanning electron microscopy (SEM). The cylindrical specimens with a 4.6 mm diameter were prepared and freeze-dried. For SEM analysis, the specimens cryogenically fractured in liquid nitrogen and, the fractured cross-section of the gels were coated with a thin layer of Gold and Palladium (Au-Pd) in a Quorum SC7620 equipment (Quorum Technologies). The morphology of hydrogel cross-sections were taken by the FEI Quanta FEG 250/Czech Republic equipment.

4.4 Mechanical Tests

The uniaxial tensile and compression tests were applied to just prepared hydrogels at 23±2 °C using a Zwick Roell Z0.5 TH test machine equipped with a 500 N load cell. Uniaxial compression tests were conducted on cylindrical gel specimens of 4.6 mm in diameter. To make thorough contact between the gel and plates before the test initial compressive contact of 0.01 N was made and gels were compressed with a strain rate of $1min^{-1}$.

The forces per original (undeformed) and actual (deformed) cross-sectional area of the gel sample, denoted by the nominal σ_{nom} and true values σ_{true} of stress respectively. Supposing the hydrogel volume remains unchanged throughout deformation, the true stress σ_{true} was calculated from equation (4.1),

$$\sigma_{true} = \lambda \, \sigma_{nom} \tag{4.1}$$

where the deformation ratio λ is the ratio between the actual (deformed) length and the original (undeformed) length.

The strain ε can be described as a variation in the length of the gel specimen compared to its original (undeformed) length, i.e., $\varepsilon = \lambda - 1$ or $\varepsilon = 1 - \lambda$, for elongation and compression, respectively. The strain is additionally determined by the biaxial extension ratio λ_{biax} ($= \lambda^{-0.5}$) due to the fact that uniaxial compression corresponds to biaxial extension. Young modulus E was estimated from the slope of σ_{nom} - ε curves between 5 and 15% deformations. The area under the stress-strain curves up to the fracture point was used to calculate the fracture energy W (toughness). The fracture nominal stress σ_f was determined from the maxima in $\sigma_{true} - \varepsilon$ plots. For the tensile tests, cylindrical gel specimens of 4.6 mm in diameter and between 3 and 5 cm in length were used. The strain rate $\dot{\varepsilon}$ was 1 min^{-1} and the initial sample length between jaws was 10±0.1 mm. Tensile tests were performed using two different grips according to the nature of the resulting sample to prevent samples from slipping between jaws. A group of gels that are hard to deform was stretched by using 1 kN grips, while softer gels were stretched by 20 N grips.

Cyclic compression tests were conducted with five compressive cycles at a strain rate $\dot{\varepsilon}$ of 1 min^{-1} up to a constant maximum strain ε_{max} from 0 to 80 % (λ_{max} increased from 1 to 0.2), followed by unloading step to zero strain and a waiting time of 1 min, before the subsequent compressive cycle.

Cyclic tensile tests were performed with successive increasing maximum strain ε_{max} from 25 to 200 % in eight successive cycles followed by immediate retraction to zero strain. The broken bonds were anticipated to rebuild until the following stretching cycle with a 1 min waiting time between cycles. Cyclic tensile tests were also conducted.

4.5 Rheological Experiments

The rheological measurements were carried out on a Bohlin Instruments Gemini 150. To reduce evaporation, a solvent trap was used during all measurements. A Peltier system was employed to keep a constant temperature.

As-prepared hydrogel samples were immersed in an excess of aqueous 7 M urea solution at 23±2 °C for 2 weeks under stirring. In this solution, all of the terpolymer hydrogels were soluble. The homogeneous polymer solutions that had been obtained in this manner were then poured into dialysis tubes (3500 MWCO, SnakeSkin, Pierce) and dialyzed for 3 days against water, followed by an additional 3 days against 4 wt% PEG-10000 to concentrate the solution. The concentrated solution was then freeze-dried on a Christ Alpha 2-4 LDplus freeze-dryer. 20 mg of the dried terpolymers that were extracted from the hydrogels were dissolved in 2 mL of distilled water in order to measure the viscosity. A cone-and-plate geometry (cone angle = 4^{o}, diameter = 40 mm) was used to measure the viscosities of polymer solutions, obtained from solubilized hydrogels, at 25 ^{o}C over the range of shear rates $\dot{\gamma}$ 1×10^{-3} and 1×10^{2} s^{-1}. The elastic modulus G' (filled symbols) and viscous modulus G'' (open symbols) of the same terpolymer solutions were measured as a function of the angular frequency ω at the strain γ_0 of 10%.

5. RESULTS and DISCUSSION

5.1 Comonomer Effect

Multiple H-bonds can easily form between H-bonding acceptor and donor functional sites of suitable polymer chains by yielding extraordinary mechanical strength. In previous study, we showed that although an aqueous solution of 60 wt% AMPS is saturated, a liquid monomer namely DMAA could be dissolved in this solution to increase the total monomer concentration [18]. Copolymerization of this solution results in physical hydrogels with improved mechanical qualities. In the present study, alternative comonomers namely methacrylic acid (MAAc) and acrylic acid (AAc) were also used in the preparation of AMPS-based hydrogels.

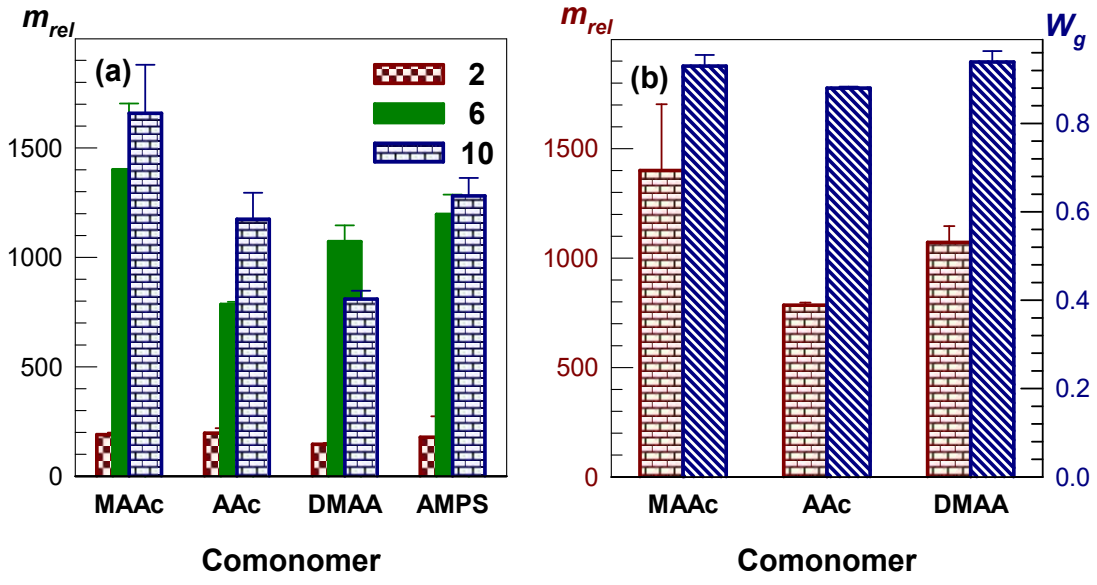

Figure 5.1 : (a) Swelling ratios (m_{rel}) of AMPS-based hydrogels in aqueous solutions at pH values of 2, 6, 10. (b) Swelling ratios (m_{rel}) and gel fractions (W_g) of AMPS-based hydrogels in pure water (pH = 6).

Swelling tests were conducted to as-prepared AMPS-based copolymer hydrogel specimens in deionized water and aqueous solutions with various pH values. Swelling ratios of hydrogels at various pH values, swelling ratios and gel fractions of copolymer hydrogels in deionized water are shown in Figure 5.1. Swelling ratios of AMPS

hydrogel at 62.5 wt% (the solubility limit of AMPS) are presented in Figure 5.1a, to express the effect of AMPS on swelling. We observed that the swelling ratio of AMPS hydrogel was high between pH = 3-10, but drastically decreased at pH = 2.

At pH = 2, swelling ratio for all gels was found to be between 150 and 200, while at pH = 6 (deionized water medium) it was between 800 and 1400. On the other hand, the gel containing MAAc can swell 1658 times its original mass at pH=10, while the equilibrium weight swelling values for AAc and DMAA are 1174 and 809, respectively. Similarly, AMPS-based hydrogels containing MAAc and AAc swelled more under alkaline conditions (pH =10). Carboxyl functional groups were responsible for high swelling values.

As shown in Figure 1b, gel fractions (W_g) are above 0.9 for all gels, meaning that water-insoluble and stable physically cross-linked hydrogels were synthesized.

Tensile stretching tests were conducted for copolymer hydrogels. heir stress-strain curves and mechanical properties are presented in Figure 5.2.

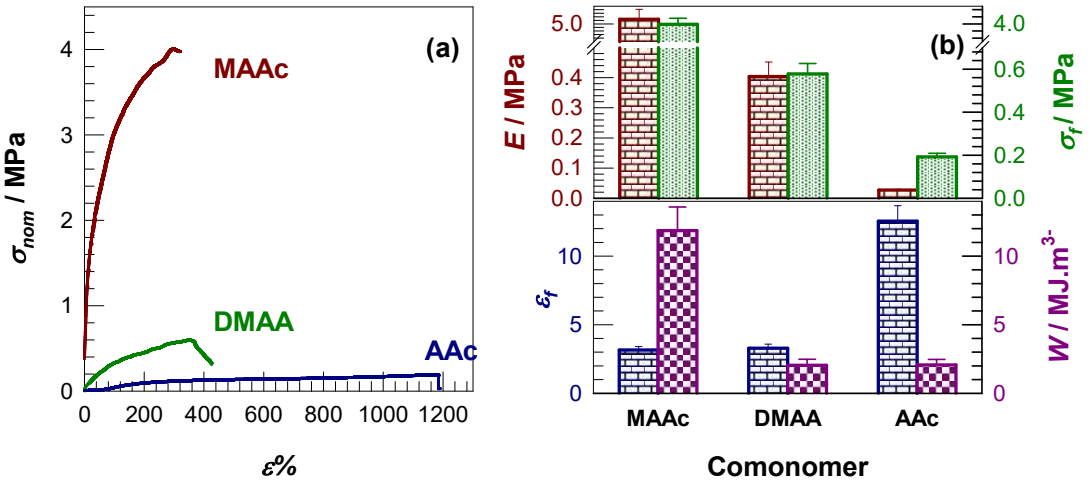

Figure 5.2 : (a) Stress-strain curves of AMPS-based hydrogels generated by using different comonomers. The amount of water at gel preparation (w) = 25 wt %. Strain rate $\dot{\varepsilon}$ = 1 min^{-1}. (b) Variations in mechanical parameters depending on the comonomer used. E = Young's modulus, σ_f = fracture stress, ε_f = fracture strain, W = toughness.

The mechanical parameters, namely, the fracture strain ε_f, fracture stress σ_f, toughness W, and Young's modulus E, of the hydrogels are displayed in Figure 5.2b plotted against comonomers used in the formation of AMPS-based hydrogels. The replacement of DMAA with methacrylic acid (MAAc) as a comonomer of AMPS did

not change the fracture strain, but the modulus and fracture stress increased 10 times and reached 5 and 4 MPa, respectively. This enormous increase in mechanical properties is also reflected in the toughness of AMPS/MAAc hydrogel which increased 6 times as compared to AMPS/DMAA hydrogel.

These experiments revealed that the replacement of DMAA with MAAc in the copolymer hydrogels significantly improves the mechanical properties while maintaining their superabsorbent behavior. After this part, we investigated how the mechanical performance of superabsorbent AMPS/DMAA hydrogels varies by replacing the DMAA with the combination of DMAA and methacrylic acid (MAAc), which are H-bond donor and H-bond acceptor molecules, respectively.

5.2 Effect of Comonomer Composition

Figure 5.3a illustrates the stress-strain curves of terpolymer hydrogels prepared at w = 25 wt% and at different MAAc contents x_{MAAc}. Data for AMPS/DMAA and AMPS/MAAc copolymer hydrogels are represented by the curves labeled by 0 and 1, respectively. It is seen that the terpolymer hydrogels with $x_{MAAc} > 0.4$ display a significantly higher fracture stress σ_f with respect to the copolymer gels, and it approaches to a maximum value of around 10 MPa at x_{MAAc} = 0.70-0.80.

The mechanical parameters, namely, the fracture stress σ_f, strain ε_f, toughness W and Young's modulus E of the hydrogels are shown in Figure 5.3b plotted against x_{MAAc}. A notable increase in all mechanical parameters has been noticed when MAAc is included into the gel network. The hydrogels' Young's modulus E first increases with increasing MAAc content and then decreases after reaching a maximum value of 26±2 MPa at x_{MAAc} = 0.80 [44,94]. After the incorporation of MAAc units, the maximum modulus is 63-fold increased compared to the AMPS/DMAA hydrogel, which can be related to a significant strengthening of H-bonding interactions in AMPS/DMAA hydrogels. Our research group recently performed theoretical calculations on similar hydrogels [18]. The results show that the hydrophobicity of MAAc units and formation of strong H-bond nanoaggregates during their copolymerization with DMAA are mainly responsible for the maximum strength of the resulting hydrogels at a critical composition of x_{MAAc} = 0.80 deviating from equimolar compositions. This implies the presence of consecutive H-bond donor and acceptor monomer units on adjacent

copolymer chains, providing cooperative H-bonding [94]. A similar trend is observable for the fracture stress σ_f and toughness W of the hydrogels exhibiting maximum values of 11±1 MPa and 31±5 MJ·m^{-3} at x_{MAAc} = 0.70 and 0.80, respectively (Table A.1).

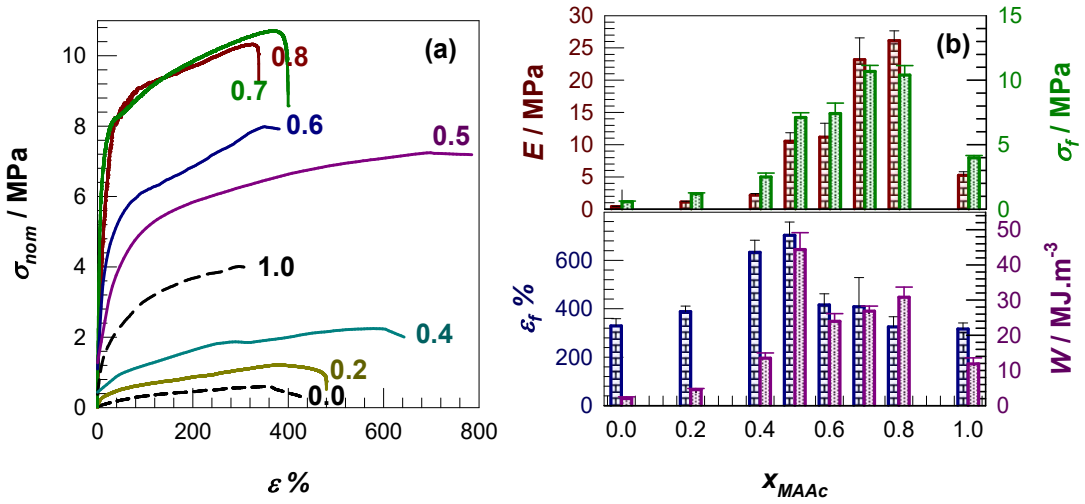

Figure 5.3 : (a) Stress-strain curves of terpolymer hydrogels generated at various x_{MAAc}. (b) Young's modulus E, the fracture stress σ_f and strain ε_f, and toughness W of the hydrogels plotted against x_{MAAc}. Strain rate $\dot{\varepsilon}$ = 1 min^{-1}.

When hydrogel specimens were placed in an excess of water during a period of two months, all hydrogels swell greatly but retain their structure without dissolving. The filled symbols in Figure 5.4a represent the gel fraction W_g, which is the mass ratio of the water-insoluble polymer to the initial mass of dried hydrogel. All the hydrogels including the copolymer hydrogels display a W_g between 0.64 and 0.94 with a minimum at x_{MAAc} = 0.60, at which the swelling ratio m_{rel} reaches a maximum value of 2900±130. Note that AMPS/DMAA and AMPS/MAAc copolymer hydrogels are represented by x_{MAAc} = 0 and 1, respectively. The terpolymer hydrogels exhibit a higher degree of swelling respect to the copolymer hydrogels. For instance, their equilibrium weight swelling ratios m_{rel} were between 1070 and 2900 refering their superabsorbency because of the strong polyelectrolyte AMPS units. Figure 5.4c presents images of a terpolymer hydrogel sample produced at x_{MAAc} = 0.80 before (left) and after (right) equilibrium swelling in water to demonstrate the superabsorbancy of the terpolymer hydrogels. The hydrogel absorbs 2035±255 times its mass in water at equilibrium during which only 10% of the polymer dissolves (W_g = 0.9).

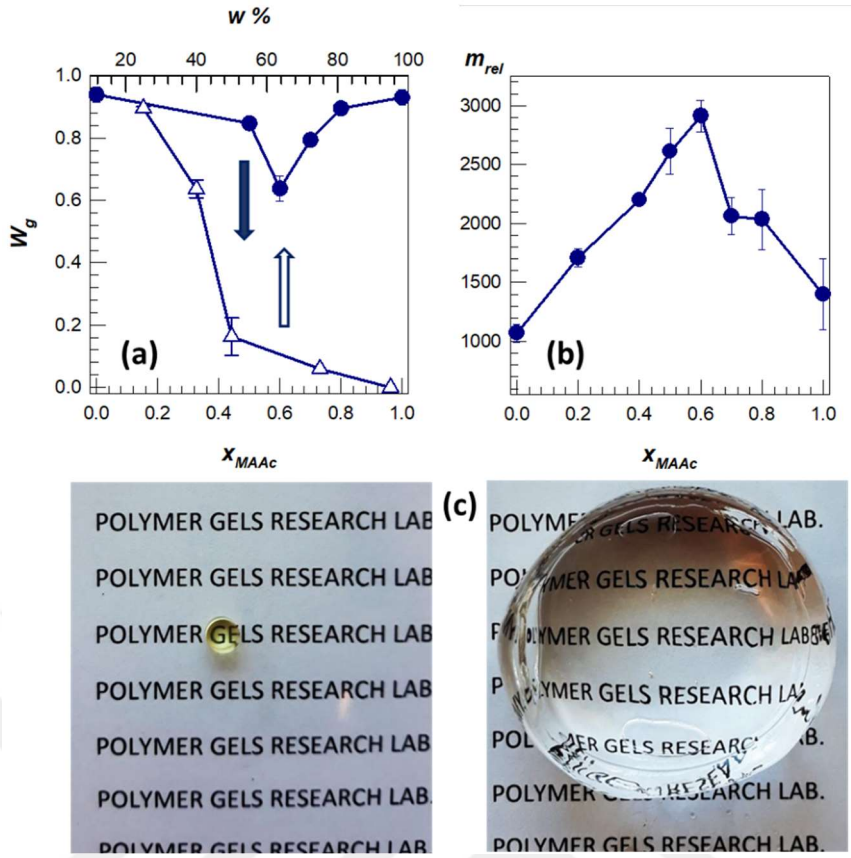

Figure 5.4 : (a) The gel fraction W_g of terpolymer hydrogels plotted against x_{MAAc} (circles) and w % (triangles). (b) Equilibrium weight swelling ratio m_{rel} of the hydrogels plotted against x_{MAAc}. (c) The images of a hydrogel sample prepared at w = 25 wt% and x_{MAAc} = 0.80 as-prepared state (left) and after swelling in water (right).

5.3 Effect of Water Content

In this section, we fixed x_{MAAc} at 0.8, at which a maximum modulus was observed, and increased the water content (w) from 25 to 95 wt% to highlight the impact of water content on the hydrogel properties. Figure 5.5a, shows the stress-strain curves and mechanical parameters of the terpolymer hydrogels formed at different w. Because of the critical change in the mechanical strength of the hydrogels depending on w, the data are also presented in a semi-logarithmic plot in Figure 5.5b.

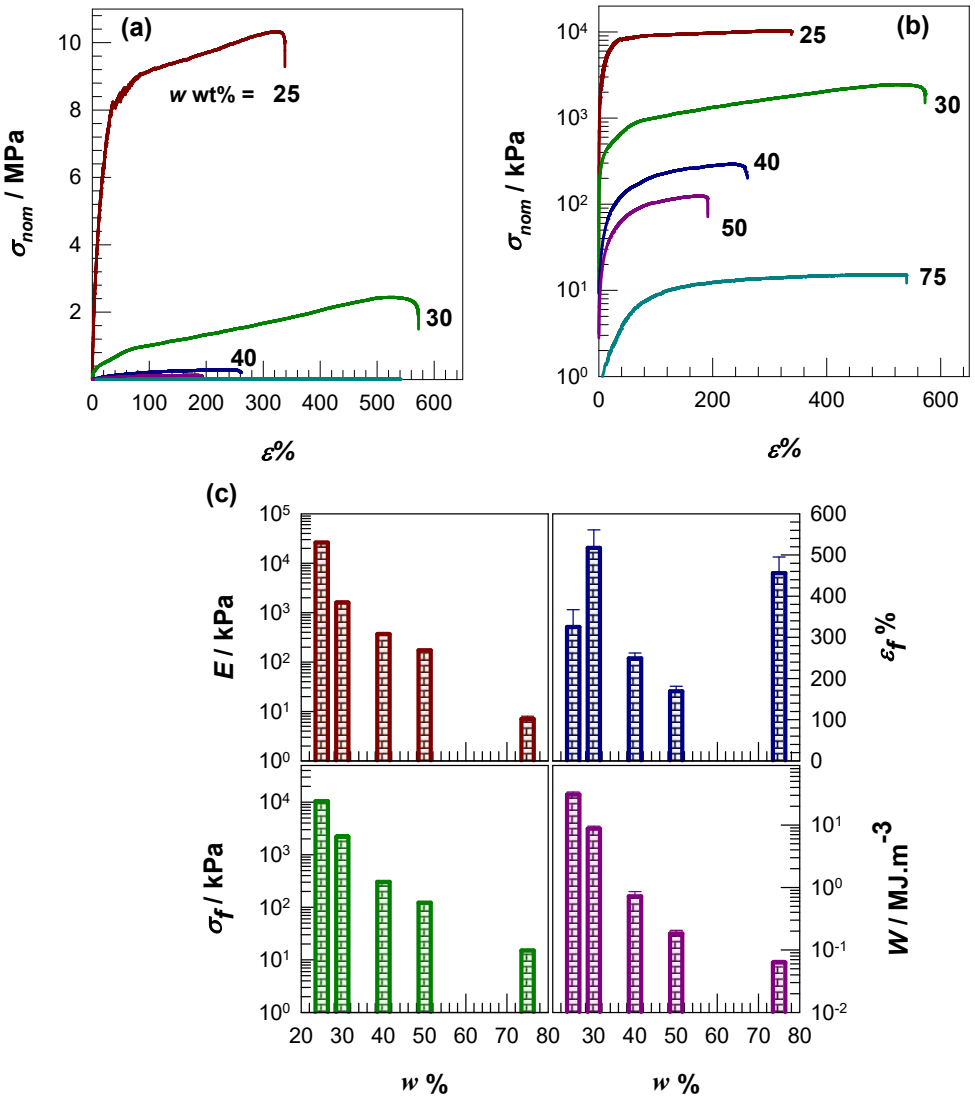

Figure 5.5 : (a) Stress-strain curves in linear and (b) semi-logarithmic scale. (c) Mechanical parameters of terpolymer hydrogels prepared at various w. Strain rate $\dot{\varepsilon} = 1\ \text{min}^{-1}$.

As a result of increasing w from 25 to 75 wt%, the modulus E and fracture stress σ_f both decrease by three orders of magnitude (from 26±2 MPa to 7±1 kPa, and 10.4±0.7 MPa to 15±1 kPa, respectively) (Table A.2). Simultaneously, solubility tests revealed that the gel fraction W_g decreases from 90±1 to 6±2% as w increases from 25 to 75 wt%, and finally the hydrogels become soluble at $w = 95$ wt% (open symbols in Figure 5.4a). The drastic decrease in the stiffness and strength of the hydrogels is additionally demonstrated in Figure 5.7 illustrating the images of cylindrical hydrogel specimens prepared at $w = 75$ (b) and 30 wt% (c). The hydrogel prepared at $w = 75$ wt% already deforms under the gravity and can be 4 times stretched under a mass of 50 g, whereas

the one that prepared at w = 30 wt% maintains its length under the same load, and withstands a load of 15 kg.

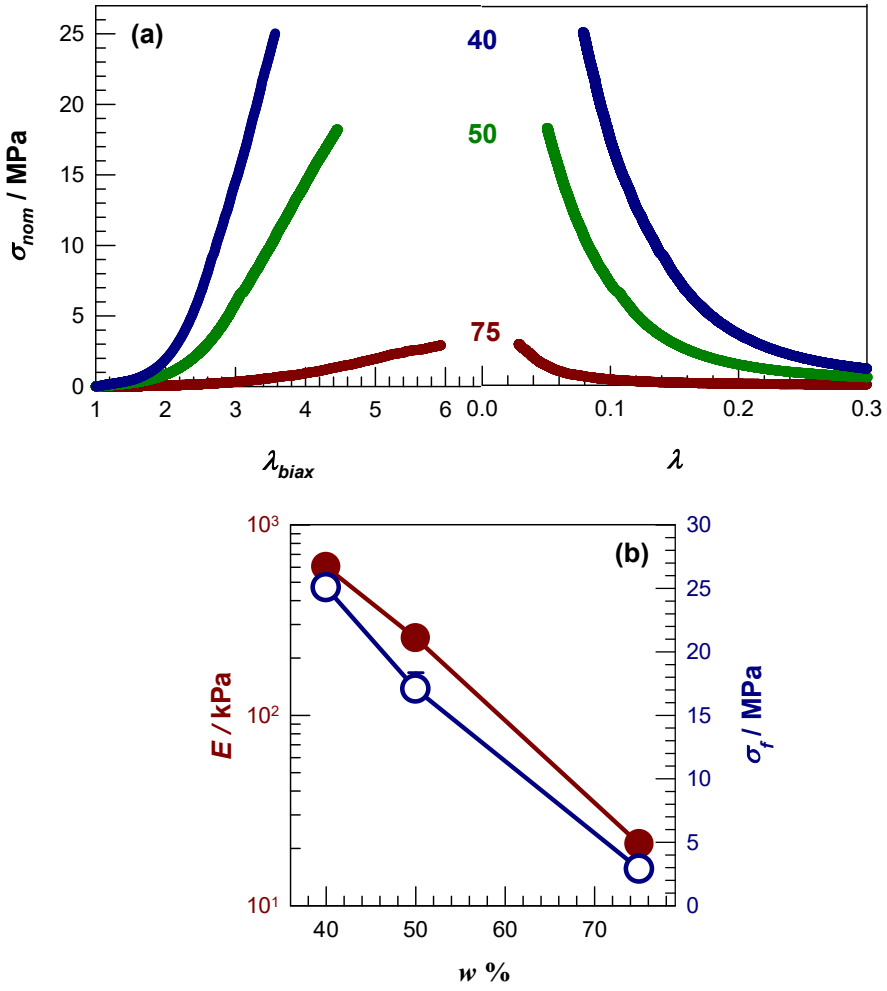

Figure 5.6 : (a) Compressive stress-strain curves of w = 40, 50, and 75 wt% hydrogels, and (b) Young modulus E (filled symbols), fracture stress σ_f (open symbols) of the hydrogels shown as a function of w.

Tensile tests were conducted by using two different grips, a group of hydrogels formed at w = 25, 30, and 40 wt% were stretched by using 1 kN grips, while other hydrogels formed at w = 75 and 50 wt% were stretched by 20 N grips. Compression tests were also applied to samples to compare with tensile test results.

The hydrogel formed at w = 25 wt% exceeds the strength of load cell during the compression test. Figure 5.6a demonstrates compressive stress-strain curves of the hydrogel samples formed at w = 75, 50, and 40 wt%, where the nominal stress σ_{nom} is plotted against the biaxial extension ratio λ_{biax} and deformation ratio λ. The Young's

modulus E and fracture nominal stress σ_f of the hydrogels are plotted against the water content w in Figure 5.6b.

The strong-to-weak transition in mechanical properties because of the decrease in the crosslink density was accompanied with a transparent-to-opaque transition in hydrogels followed by a phase separation (Figure 5.7a). The hydrogels formed at $w \leq$ 40 wt% were transparent while they became translucent at w = 50 wt% and finally opaque at w = 75 wt%. Further increase in w to 95 wt% resulted in a phase-separated system consisting of a viscous solution and opaque gel. The occurrence of phase separation was also checked by scanning electron microscopy (SEM). SEM images of the specimens freeze-dried under identical conditions reflected the appearance of a phase-separated structure and hence, a macroporous structure as the water content at the gel preparation is increased (Figure A.1)

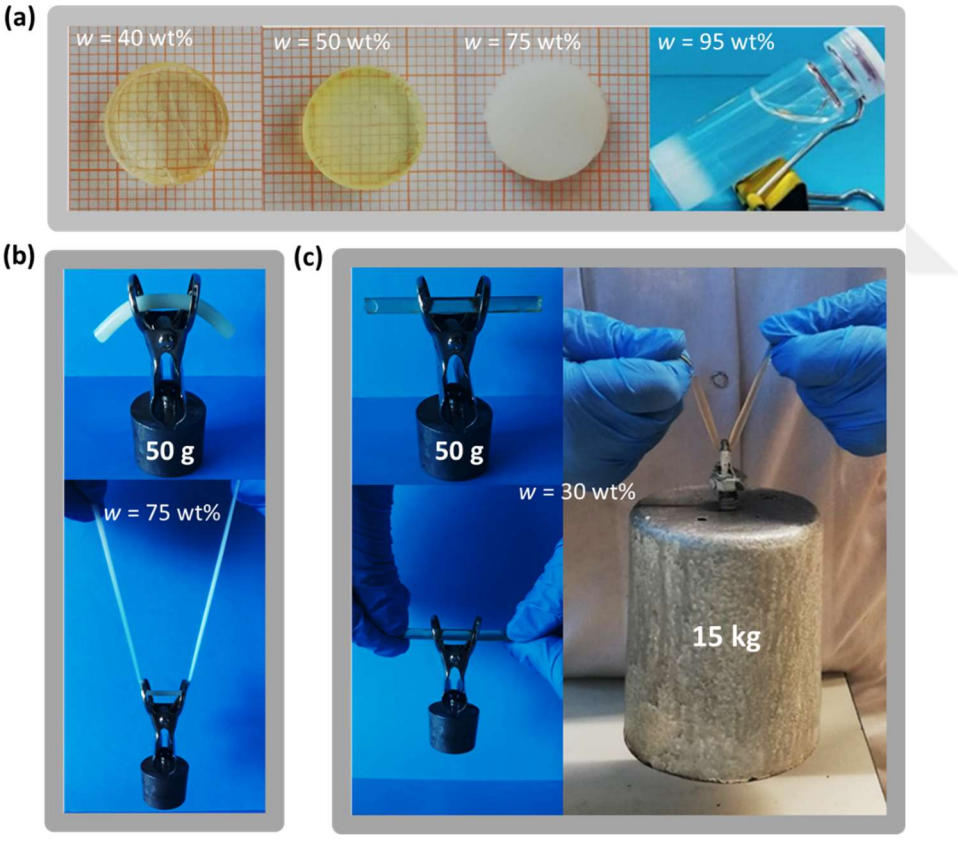

Figure 5.7 : (a) Images of hydrogels prepared at different water contents are presented. (b, c) Images of hydrogel specimens prepared at (b) w = 75 and (c) 30 wt% under the gravity and under load stated.

5.4 Solubilization of the Hydrogels

The question thus may arise what are type of the crosslinks in the hydrogels making them stable in water? Given that DMAA units are capable of self-cross-link, it is possible to assume that some chemical crosslinks may develop in the hydrogels. [44,95]. The solubility tests were performed on as-prepared hydrogels in aqueous solutions of urea which is a well-known H-bond breaking agent.

All the hydrogels generated at various x_{MAAc}, and w could be dissolved in 7 M urea solutions within 2 weeks reflecting their physical nature. Considering H-bonds are much weaker than covalent bonds, this experiment also indicates the existence of multiple H-bonds between the terpolymer chains strengthening the interchain interactions. It should be noted that the chain entanglements may strengthen the H-bonding interactions by limiting the mobility of the terpolymer chains [96].

The complete solubilization of the terpolymer hydrogel with 25 wt% water required at least 2 weeks under stirring while the hydrogels with a higher water content could be dissolved in a much shorter time. To characterize the microstructure of the hydrogels generated at different water contents, solubilized hydrogels were transfered into dialysis tubes (3500 MWCO, Snake Skin, Pierce) and dialyzed for 3 days against water to remove urea by replacing water several times and another 3 days against aqueous PEG-10000 solution (4 wt%) to increase the concentration of the obtained terpolymer solutions. The concentrated polymer solutions were finally freeze-dried to obtain terpolymers forming the primary chains. It should be noted that the gel region of the phase-separated hydrogel generated at w = 95 wt% was isolated from the supernatant viscous solution and then solubilized. Figure 5.8a presents the viscosities η of aqueous terpolymer solutions, each at 1 w/v% concentration, plotted against the shear rate $\dot{\gamma}$. Viscosity is observed to increase with decreasing water content w, revealing the production of longer primary chains at greater monomer concentrations during gelation. The frequency (ω) sweep results of the same solutions isolated from hydrogels with w = 75, 50, and 25 wt% are shown in Figure 5.8b. To prevent overlapping, the storage modulus G' and loss modulus G'' data are vertically shifted by a factor of k. The graphic illustrates the normal behavior of a semidilute solution: G'' is greater than G' at low frequencies, but G' and G'' cross at a frequency at which the behavior changes from more liquid-like to solid-like. The crossover frequency ω_c

decreases from 26 to 15 s^{-1} with decreasing w from 75 to 25 wt% which is an indication of increasing amount of interchain H-bonds linking the primary chains. The findings indicate that when compared to opaque hydrogels, transparent hydrogels formed at $w \leq 40$ wt% have longer polymer chains with a higher number of intermolecular H-bonds The increasing number of H-bonds with increasing chain length can be explained with the proximity effect [96–98]. Thus the preformed H-bond that links two polymer chains limits the mobility of the chain units close to the initial bond and hence facilitates the formation of subsequent H-bonds.

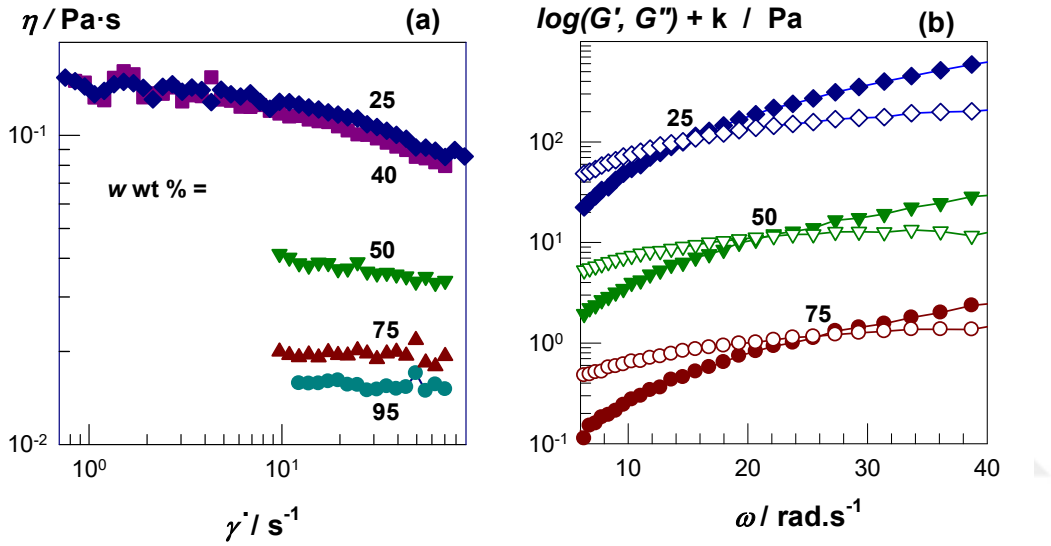

Figure 5.8 : (a) The shear rate $\dot{\gamma}$ dependence of the viscosities η of aqueous terpolymer solutions isolated from hydrogels prepared at w indicated. Polymer concentration of 1 w/v %. Temperature = 25 °C. (b)The storage modulus G' (filled symbols) and loss modulus G'' (open symbols) of the same terpolymer solutions plotted against the angular frequency ω. The vertical shift factor k = 0, 1, and 2 for w = 25, 50, and 75 wt%, respectively. γ_0 = 10%.

A strong H-bonded complex formed between MAAc and DMAA units, which is unable to absorb all of the water in the hydrogel, may be the cause of the formation of opacity and, eventually, phase separation with increasing water content [94]. A phase separation occurs when a gel separates from the solution phase because the water absorption capacity of highly H-bonded and, thus, highly crosslinked regions will be lower than that of the loosely crosslinked regions. The opaque phase-separated gel in equilibrium with the viscous polymer solution was clearly seen to behave in this way for the hydrogel generated at w = 95 wt% (Figure 5.9a); it does not flow and regains its shape and size after shaking. To reveal the composition of the polymer chains in

the gel and sol phases, FTIR and elemental microanalysis experiments were performed on dried samples taken from both phases. Figure 5.9b shows amide I region of the FTIR spectra of solution (up) and gel phases (down). The C=O stretching vibrations of AMPS units in the sol and gel appear at 1635 and 1647 cm^{-1}, respectively, where the strong absorption peak for the sol reveals that it is rich in AMPS units. The C=O stretching of MAAc units appears at 1704 and 1693 cm^{-1} for sol and gel respectively. The absorption peak for the DMAA units cannot be detected in FTIR spectra although it appears in physical PDMAA hydrogels formed at w = 50 wt% and under identical conditions at 1603 cm^{-1} (Figure A.2).

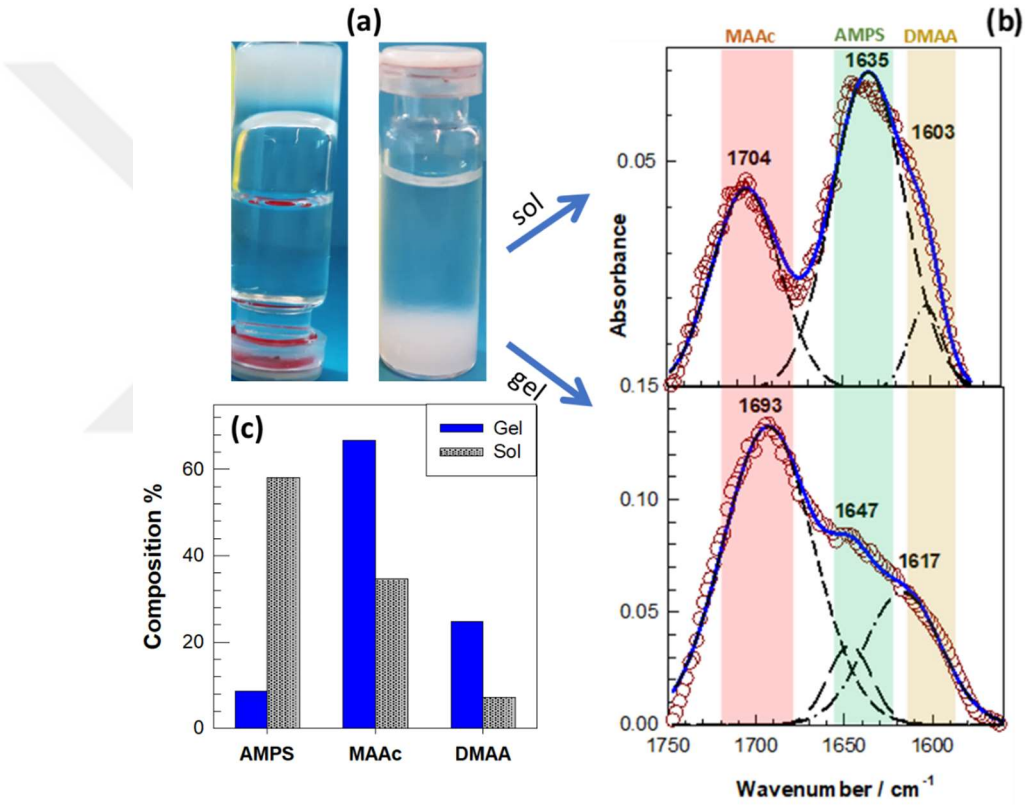

Figure 5.9 : (a) The images of the phase-separated hydrogel. w = 95 wt%. (b) amide I region of the FTIR spectra of solution (up) and gel phases (down) of the phase-separated hydrogel. The open symbols and blue solid curves present original and fitted spectra while black dashed lines are hidden peaks for MAAc (dashed), AMPS (long dash), and DMAA units (dash-dot). (c) The composition of the terpolymers in the sol and gel phases of the phase-separated hydrogel.

To estimate the composition of the terpolymers in the gel and sol phases, their spectra were investigated using PeakFit software. The band was deconvolved by Gauss Amplitude function, after linear baseline correction was made to the amide I region (1560−1750 cm^{-1}). For the curve fitting procedure, the peak positions of MAAc and

AMPS were fixed, permiting peak widths and intensities to shift. The position of the hidden peak of DMAA was varied to obtain a good fit to the spectra of the terpolymer with an r-squared value above 0.98. The open symbols and blue solid curves in Figure 5.9b present original and fitted spectra while black dashed lines are hidden peaks for MAAc (dashed), AMPS (long dash), and DMAA units (dash-dot). The composition of the terpolymers is estimated from the area of the peaks and presented in Figure 5.9c. It is seen that the terpolymer in the sol phase consists of 58 mol % AMPS compared to 9 mol % in the gel phase. In contrast, the terpolymer in the gel phase is rich in both MAAc and DMAA units with a MAAc mole fraction (x_{MAAc}) of 0.73.

Elemental analysis for C, N, and S were conducted on phase-separated hydrogels prepared at w = 95 and 93 wt% to determine the composition of the terpolymers in both phases. Among the monomers we used, only AMPS contains sulphur atom, while both AMPS and DMAA contain nitrogen atoms, but both sulphur and nitrogen atoms do not exist in MAAc. The distribution of the monomers in gel and sol phases was calculated from elemental microanalysis and shown in Figure 5.10b and Table A.3 and A.4.

The sol phase of both hydrogels contains about 37 mol% AMPS compared to 12-23 mol% in the gel phase, which appears to be the reason for the water solubility of the sol phase, due to the osmotic pressure of AMPS counterions domineering the elastic response of physical cross-links,

The gel phase is mostly composed of MAAc units (64-78 vs 43-46 mol% in the sol) resulting in a simultaneous increase in MAAc mole ratio (x_{MAAc}) to 0.83-0.89. As seen in Figure 5.3b, such a x_{MAAc} value produce mechanically strongest hydrogels at w = 25 wt%. Accordingly, the phase separation is formed owing to the development of H-bonded complex between DMAA and MAAc units of the hydrogels while AMPS-rich polymer chains remain in the solution phase.

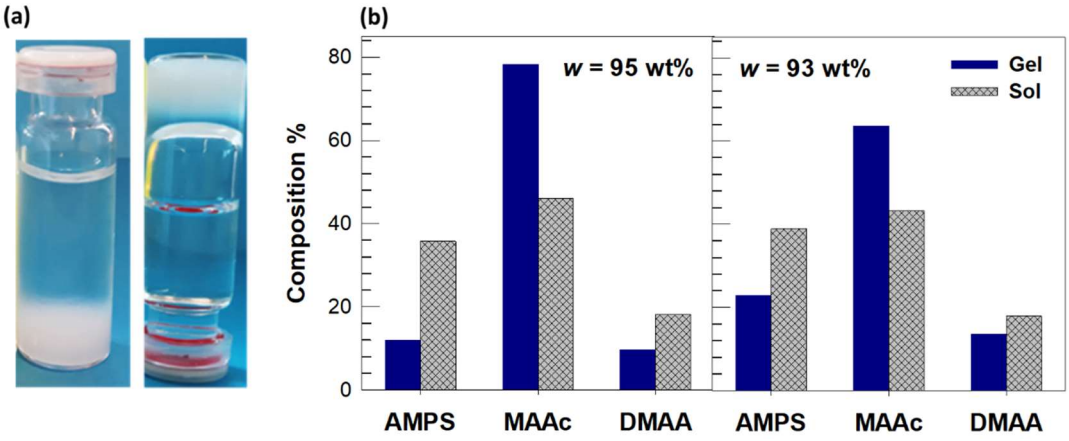

Figure 5.10 : (a) The images of the phase-separated hydrogel. w = 95 wt%. (b) The composition of the terpolymers in the sol and gel phases of the phase-separated hydrogel formed at w = 95 and 93 wt%.

5.5 Time-dependent Properties of the Hydrogels

Because all the hydrogels reported here are formed via H-bonding interactions, their mechanical properties reported above should depend on the time scale of the experimental window. Figure 5.11a demonstrates stress-strain curves of the hydrogel formed at w = 30 wt% and x_{MAAc} = 0.80 at various strain rates $\dot{\varepsilon}$ indicated. In Figure 5.11b, the modulus E and fracture stress σ_f are presented against the strain rate $\dot{\varepsilon}$. Both E and σ_f increase with increasing $\dot{\varepsilon}$, i.e., with decreasing time scale as expected for physical hydrogels. For each stress-strain curve in Figure 5.11a, the stress at which the curve becomes noticeably nonlinear is designated as σ_y. Moreover, the yield stress σ_y also increases with $\dot{\varepsilon}$ and shows a linear dependence when plotted against log ($\dot{\varepsilon}$) (Figure 5.11c), which is in accord with the estimation of the Eyring model of mechanically driven decomposition of molecular bonds [99–101],

$$\sigma_y = \frac{2\mathrm{kT}}{V_a} (\ln \dot{\varepsilon} / \varepsilon_0) + \frac{2E_a}{V_a} \qquad (5.2)$$

where k is the Boltzmann constant (R/N_A), T is the absolute temperature (296±2 K), V_a is the activation volume, ε_o is the pre-exponential factor, and E_a is the activation energy. The solid line in Figure 5.11c is the best fit of the experimental σ_y vs $\dot{\varepsilon}$ data to Equation 5.2 yielding the activation volume V_a as 18±1 nm^3 /molecule. This volume can be thougth of the volume of the polymer units in the hydrogels engaged in the cooperative motion that results to yielding. V_a is much larger than the covalently cross-linked systems but close cellulose acetate system and semicrystalline hydrogels with

= 17.4 and 12-13 nm^3 /molecule, respectively [44,102–106]. This reveals activation of larger species in the hydrogels during deformation.

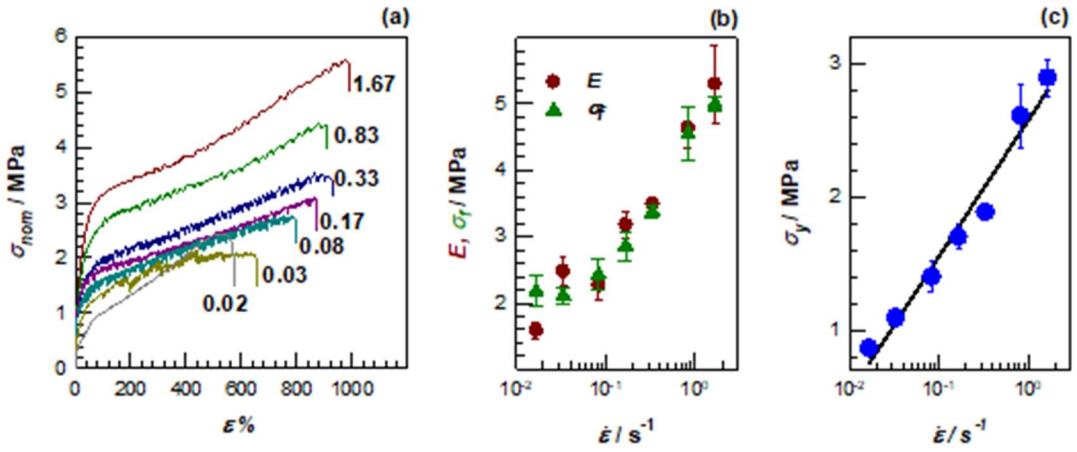

Figure 5.11 : (a) The stress-strain curves of the hydrogel prepared at w = 30 wt% and x_{MAAc} = 0.80 at different strain rates $\dot{\varepsilon}$ (min^{-1}) indicated. (b) The modulus E and fracture stress σ_f plotted against $\dot{\varepsilon}$. (c)The yield stress σ_y shown as a function of log ($\dot{\varepsilon}$). (c) The line is the best fit for the data.

5.6 Large Strain Behaviour

For a better comprehension of the nature of H-bonds in terpolymer hydrogels, their large strain behaviour was examined by cyclic compression and tensile tests. The tests were conducted at a constant strain rate $\dot{\varepsilon}$ of 1 min^{-1}. The waiting time between cycles for recovery of the broken bonds was fixed at 1 min. Figure 5.12a presents five successive loading and unloading cycles applied on hydrogels prepared at w = 75, 50, and 40 wt%. Each cycle consists of a loading step (solid lines) up to a maximum strain ε_{max}= 80% followed by the unloading step (dashed lines) to zero strain. The unit of the strain in the figure is presented by the deformation ratio λ (1 − ε). In an ideal case, the stress-strain curve of the unloading should follow the loading curve since there is no mechanical energy dissipation in a perfectly elastic material. The deviation between the loading and unloading routes reflects the presence of energy dissipation under strain. In Figure 5.12a, it is seen that the unloading curve deviates from the previous loading, indicating some interchain bonds in the hydrogel are broken.

The trend observed in cyclic compression for a fixed ε_{max} indicating the existence of energy dissipation is that the unloading curve of each cycle deviates from the loading curve, with less area under the curve. The fact that each loading curve follows the same

path as the former loading curve indicates that the broken bonds are restored in a 1-minute waiting period.

The filled symbols in Figure 5.12b express the hysteresis energies U_{hys} of the hydrogels determined from the area between the loading and unloading curves using the equation:

$$U_{hys} = \int_0^{\varepsilon_{max}} \sigma_{nom}\, d\varepsilon \; - \int_{\varepsilon_{max}}^{0} \sigma_{nom}\, d\varepsilon \tag{5.2}$$

Keep in mind that the overall amount of bonds broken during compression up to the maximum is closely correlated with the hysteresis energy U_{hys} [10,105]. A semi-logarithmic plot was used to compare the hysteresis energies of gels prepared at different concentrations. In the figure, it could be seen that increasing total monomer concentration, significantly increases hysteresis energy, and the bonds are reversibly broken under strain.

The open symbols in Figure 5.12c represent the fraction of dissipated energies f_{diss} of the hydrogels under stress calculated by:

$$f_{diss} = \frac{U_{hys}}{\int_0^{\varepsilon} \sigma_{nom} d\varepsilon} \tag{5.4}$$

The quantity of energy dissipated per unit of loading energy, or the ratio of dissipated energy to the loading energy (f_{diss}), can be thought of as a parameter that shows how much energy is dissipated under a constant external load [18,106].

From U_{hys} values, it can be seen that after each cycle, energy of broken bonds was restored for all hydrogels and this can be confirmed with f_{diss}. For w = 40 wt% indeed, both U_{hys} and f_{diss} assume constant values, 191±9 kJ·m^{-3} and 0.40±0.01, respectively. The reversibility of the mechanical cycles remains unchanged when w is increased to 50 wt% at which a translucent hydrogel generates, while both U_{hys} and f_{diss} decreases, i.e., less energy is dissipated during the cycles (Figure 5.12).

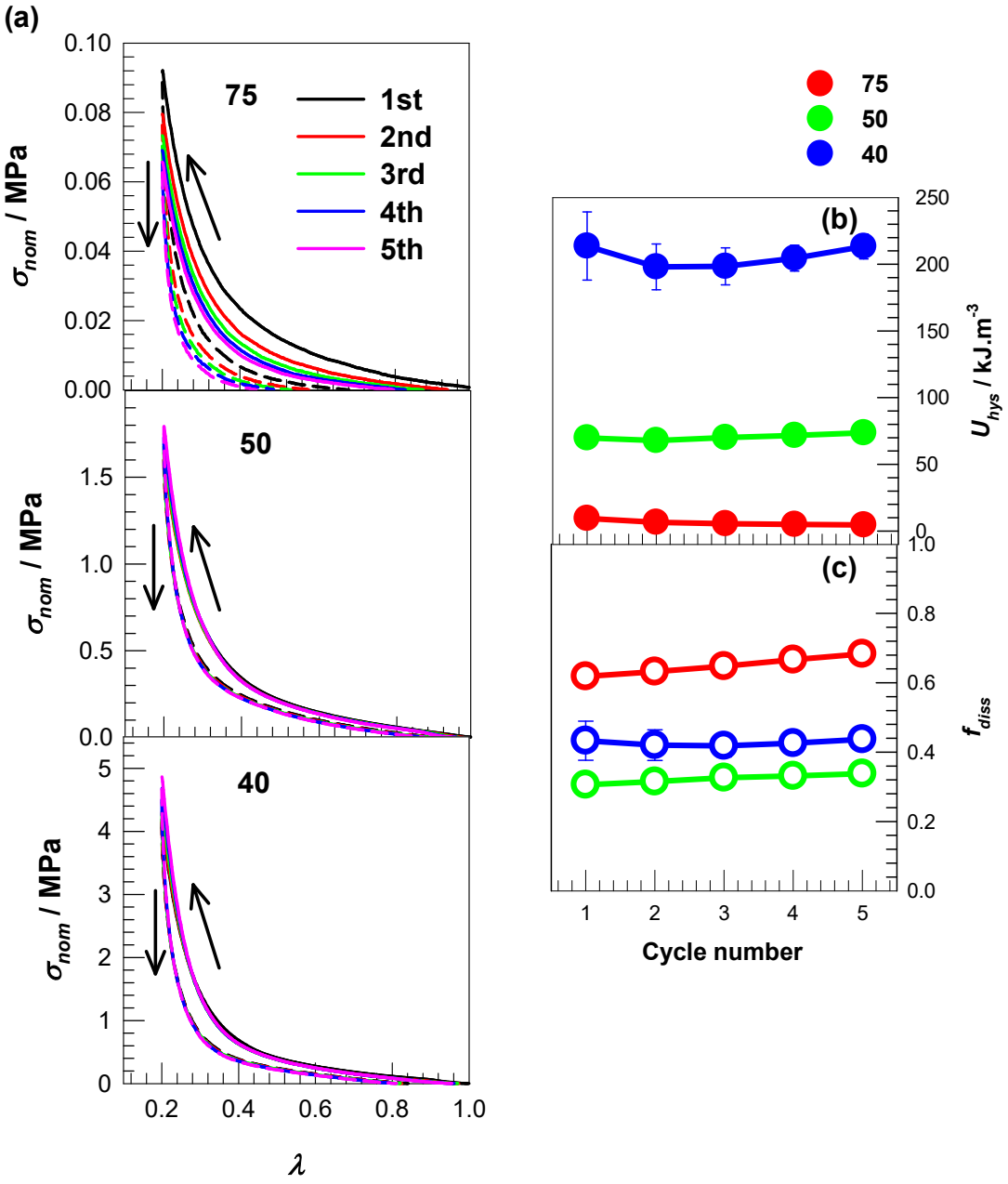

Figure 5.12 : (a) Five successive compressive cyclic tests were applied on hydrogels formed at w = 40, 50, and 75 wt% up to a constant ε_{max} of 80%; $\dot{\varepsilon}$ = 1 min^{-1}. (b) Hysteresis energy U_{hys} (filled symbols) and (c) the ratio of dissipated energy per loading energy f_{diss} (open symbols) data of hydrogels prepared at w = 40, 50, and 75 wt% plotted against the number of cycles. Loading and unloading are denoted in (a) by the up and down arrows, respectively.

The cyclic tensile tests were performed on hydrogel specimens prepared at w = 25, 40, 50, and 75 wt% with increasing maximum strain ε_{max} from 25 to 200% in eight successive cycles. The measurements are illustrated in Figure 5.13a where the loading and unloading curves are presented by solid and dashed lines, respectively.

Here again, all the loading curves follow the stress-strain curve of the virgin sample (Figure A.3). The hydrogels recover to their initial sizes until the subsequent loading with a 1 min waiting time between cycles. A semi-logarithmic plot was used to compare the hysteresis energies of gels prepared at different concentrations. Both U_{hys} and f_{diss} increase with decreasing w and ε_{max} reflecting the presence of a higher amount of H-bonds.

As seen in Figure 5.13b, U_{hys} increases as w decreases or ε_{max} increases. This situation reflects the increased level of repairable damage in the hydrogels. The fraction of the loading energy dissipated during each cycle (f_{diss}) is a better parameter to compare the dissipative properties of terpolymer hydrogels produced at various water contents, because it provides the dissipated energy per loading energy thus excludes the variations in the mechanical performances of the gels. In Figure 5.13c, f_{diss} is approximately 25% and independent of ε_{max} for opaque hydrogels formed at w = 50 and 75 wt%, indicating that 25% of the loading energy is dissipated. Moreover, f_{diss} is around 60% for transparent hydrogels formed at w = 25 and 40 wt% at low ε_{max}, however as ε_{max} increases, f_{diss} decreases and nears the value of opaque hydrogels. The findings reveal that phase-separated hydrogels dissipate less energy than homogenous hydrogels. The reversibility of the cycles also indicates that microstructure of the hydrogels can recover itself after a microscopic damage. However, cut-and-heal tests revealed that the hydrogels lack the ability of autonomous healing or healing with the effect of temperature, due to their high stiffness which limits the mobility of the chains.

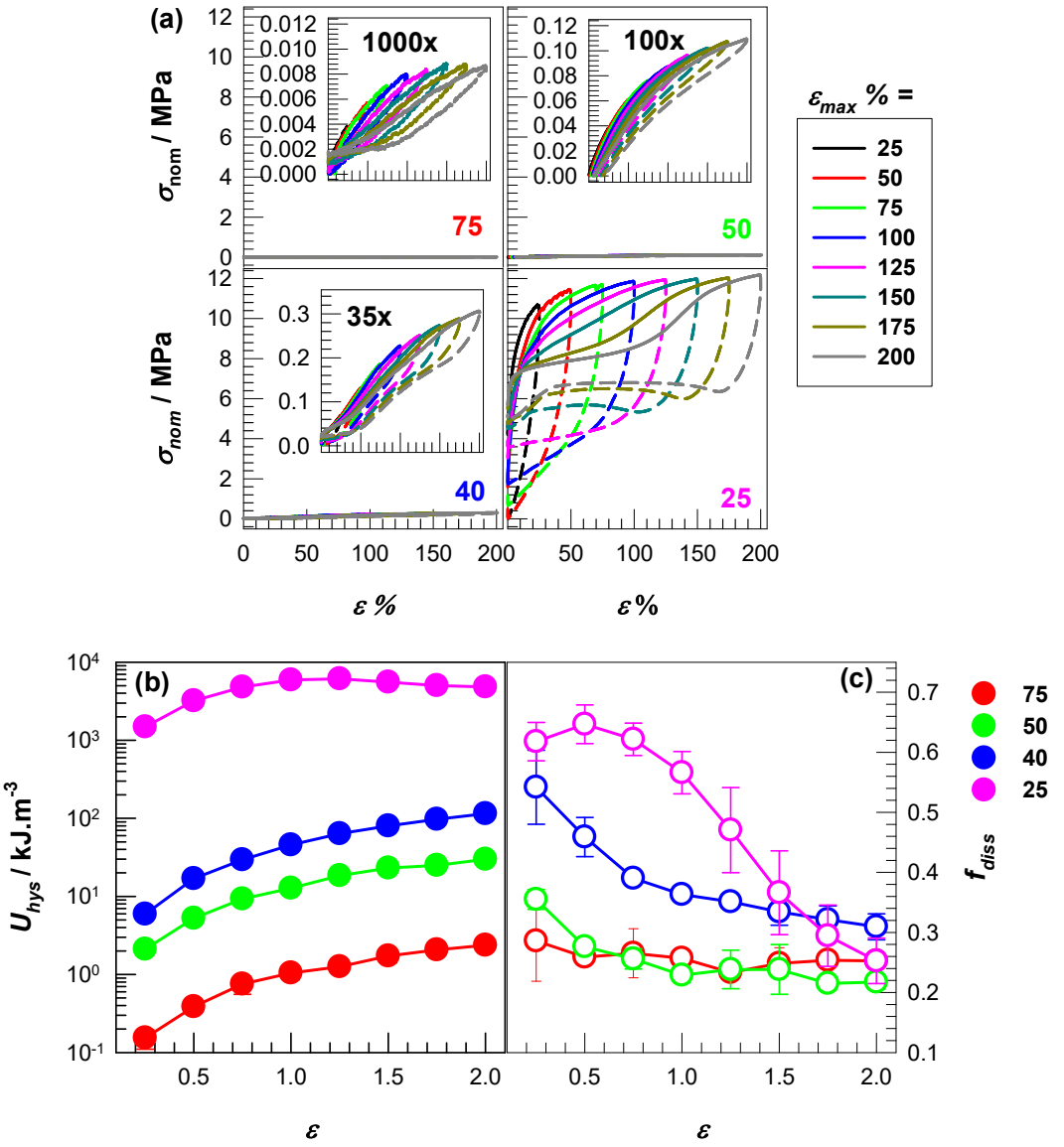

Figure 5.13 : (a) Cyclic tensile tests were applied to hydrogels prepared at w = 25, 40, 50 and 75 wt% with successively increasing ε_{max} from 25 to 200% in eight steps; $\dot{\varepsilon} = 1\ min^{-1}$. (b) Hysteresis energy U_{hys} (filled symbols) and (c) the ratio of dissipated energy per loading energy f_{diss} (open symbols) plotted against the strain obtained from these cyclic tensile test results. The solid and dashed lines in (a) represent the loading and unloading curves, respectively. To make it clear, nominal stress (y-axis) has the same scale for all gels. The insets are 35, 100, and 1000 times zoom-in of stress-strain curves of hydrogels formed at w = 40, 50, and 75 wt%, respectively.

6. CONCLUSIONS

The nature of the systems is regulated, protected, and conductive due to the presence of soluble ions and water. Hydrophilic groups are important for the permeability of metabolites, which allows appropriate water content and gives stability to typical biological processes (including endurance to the decomposition of the polymer and to reactions that are unfavorable to the organism). A hydrogel is a network of hydrophilic polymer chains that can store a large quantity of water while maintaining their structural integrity as a result of chemical or physical crosslinking of the individual polymer chains. H-bonds are required in many biological and chemical processes and are important in the creation of physical hydrogels. Cooperative H-bonding interactions linking polymer chains are necessary for the creation of robust physical hydrogels that are stable in water.

When swollen in water, the hydrogels derived from 2-acrylamido-2-methyl-1-propanesulfonic acid (AMPS) exhibit extremely high and pH-independent water absorption capacities as well as electro-sensitive properties. The goal of the present thesis was to create physical AMPS-based hydrogels and enhance their mechanical properties through the addition of the comonomers MAAc and DMAA to the H-bonded polymer network. All PAMPS hydrogels are prepared by using UV photopolymerization method.

In the first part of the thesis, liquid vinyl monomers, namely AAc, MAAc, and DMAA were used as comonomers of AMPS to increase the total monomer concentration of the precursor solutions. It was found that the inclusion of MAAc in PAMPS chains considerably boosts the mechanical performance of the resulting AMPS/MAAc copolymer hydrogels without changing their superabsorbent behaviour.

In the second part, both MAAc and DMAA at various compositions were incorporated into PAMPS hydrogels to obtain terpolymer hydrogels. In our experiments, the mole fraction of the comonomers MAAc and DMAA in the termonomer mixture was fixed at 0.62 while the mole fraction (x_{MAAc}) of MAAc in the comonomer mixture and the water content (w) of the precursor solution were varied. For the first set of terpolymer

hydrogel preparation, w was fixed at 25 wt% while MAAc content in comonomer mixture (x_{MAAc}) was varied. We observed that Young's modulus E of the hydrogels increases with increasing MAAc content and after attaining a maximum value of 26±2 MPa at x_{MAAc} = 0.80, and then decreases once again. In the second set, MAAc content in comonomer mixture (x_{MAAc}) was fixed at x_{MAAc} = 0.8 while the water content was varied between 25 and 95 wt%. The mechanical and swelling tests were conducted on terpolymer hydrogels, and their network chains were characterized by rheological studies, FTIR and microstructure elemental analyses. These results showed that the homogeneous terpolymer hydrogel with a uniform network formed at $w \leq 40$ wt% turns into a colloidal hydrogel at $w > 40$ wt%. Simultaneously, a transition from transparent to opaque in appearance was observed as the water content at gelation is increased. The results were explained with the phase separation of highly hydrogen-bonded and hence highly crosslinked regions from the loosely hydrogen bonded domains. Thus, the hydrogels prepared at $w > 40$ wt% compose of less swollen, highly H-bonded, AMPS-poor phase-separated aggregates interconnected by loosely H-bonded AMPS-rich regions. Cyclic mechanical tests revealed that homogeneous hydrogels formed at $w \leq 40$ wt% dissipate larger amount of energy as compared to the phase-separated colloidal hydrogels prepared at $w > 40$ wt %.

In conclusion, AMPS-based superabsorbent hydrogels with excellent mechanical properties were successfully synthesized. Among all hydrogels prepared in this work, the terpolymer hydrogel prepared at x_{MAAc} = 0.80 and in the existence of 25 wt% water exhibits the highest modulus E (26±2 MPa), toughness W (31±5 $MJ \cdot m^{-3}$), and the largest equilibrium weight swelling ratio m_{rel} (2035±255).

REFERENCE

[1] **Ma, J., Xiaolu Li bc, ac, & Bao ac, Y.** (2015). Advances in cellulose-based superabsorbent hydrogels. *RSC Advances, 5,* 59745-59757.

[2] **Ibrahim, S. M., Salmawi, K. M. el, & Zahran, A. H.** (2003). Synthesis of Crosslinked Superabsorbent Carboxymethyl Cellulose/Acrylamide Hydrogels Through Electron-Beam Irradiation. *Journal of Applied Polymer, 104,* 2003-2008.

[3] **Gupta, P., Vermani, K., & Garg, S.** (2002). Hydrogels: From controlled release to pH-responsive drug delivery. *Drug Discov. Today*, *7*, 569–579.

[4] **Kaşgöz, H., & Durmus, A.** (2008). Dye removal by a novel hydrogel-clay nanocomposite with enhanced swelling properties. *Polym. Adv. Technol.*, *19*, 838–845.

[5] **Kosemund, K., Schlatter, H., Ochsenhirt, J. L., Krause, E. L., Marsman, D. S., & Erasala, G. N.** (2009). Safety evaluation of superabsorbent baby diapers. *Regul. Toxicol. Pharmacol.*, *53*, 81–89.

[6] **Calvert, P.** (2009). Hydrogels for Soft Machines. *Advanced Materials*, *21*, 743–756.

[7] **Zhao, X.** (2014). Multi-scale multi-mechanism design of tough hydrogels: Building dissipation into stretchy networks. *Soft Matter*, *10*, 672–687.

[8] **Tanaka, Y., Fukao, K., & Miyamoto, Y.** (2000). Fracture energy of gels. *The European Physical Journal E. 2000 3:4*, *3*, 395–401.

[9] **Abdurrahmanoglu, S., Can, V., & Okay, O.** (2009). Design of high-toughness polyacrylamide hydrogels by hydrophobic modification. *Polymer*, *50*, 5449–5455.

[10] **Creton, C.** (2017). 50th Anniversary Perspective: Networks and Gels: Soft but Dynamic and Tough. *Macromolecules*, *50*, 8297–8316.

[11] **Gong, J. P.** (2010). Why are double network hydrogels so tough? *Soft Matter*, *6*, 2583–2590.

[12] **Zhao, S. X., & Zhao, X.** (2014). Multi-scale multi-mechanism design of tough hydrogels: building dissipation into stretchy networks. *Soft Matter*, *10*, 672–687.

[13] **Brown, H. R.** (2007). A model of the fracture of double network gels. *Macromolecules*, *40*, 3815–3818.

[14] **Gong, J. P.** (2010). Why are double network hydrogels so tough? *Soft Matter*, *6*, 2583–2590.

[15] **Creton, C., & Ciccotti, M.** (2016). Fracture and adhesion of soft materials: a review. *Rep Prog Phys*, *79*.

[16] **Fu, J.** (2018). Strong and tough hydrogels crosslinked by multi-functional polymer colloids. *J Polym Sci B Polym Phys*, *56*, 1336–1350.

[17] **Fu, J., & in het Panhuis, M.** (2019). Hydrogel properties and applications. *J. Mater. Chem B*, *7*, 1523–1525.

[18] **Su, E., Yurtsever, M., & Okay, O.** (2019). A Self-Healing and Highly Stretchable Polyelectrolyte Hydrogel via Cooperative Hydrogen Bonding as a Superabsorbent Polymer. *Macromolecules*, *52*, 3257–3267.

[19] **Staudinger, H., & Husemann, E.** (1935). Über hochpolymere Verbindungen, 116. Mitteil.: Über das begrenzt quellbare Poly-styrol. *Berichte der deutschen chemischen Gesellschaft (A and B Series)*, *68*, 1618–1634.

[20] **Staudinger, H., & Fritschi, J.** (1922). Über Isopren und Kautschuk. 5. Mitteilung. Über die Hydrierung des Kautschuks und über seine Konstitution. *Helvetica Chimica Acta*, *5*, 785–806.

[21] **Flory, P.** (1953). *Principles of polymer chemistry*, Cornell University Press, Ithaca, NY.

[22] **Dušek, K., & Patterson, D.** (1968). Transition in swollen polymer networks induced by intramolecular condensation. *Journal of Polymer Science Part A-2: Polymer Physics*, *6*, 1209–1216.

[23] **Tanaka, T.** (1978). Collapse of Gels and the Critical Endpoint. *Phys. Rev. Lett.*, *40*, 820.

[24] **Pennadam, S. S., Firman, K., Alexander, C., & Górecki, D. C.** (2004). Protein-polymer nano-machines. Toward synthetic control of biological processes. *J. Nanobiotechnology*, *2*, 1–7.

[25] **Schild, H. G.** (1992). Poly(N-isopropylacrylamide): experiment, theory and application. *Prog. Polym. Sci.*, *17*, 163–249.

[26] **Tanaka, Y., Gong, J. P., & Osada, Y.** (2005). Novel hydrogels with excellent mechanical performance. *Prog. Polym. Sci.*, *30*, 1–9.

[27] **Wichterle, O., & Lím, D.** (1960). Hydrophilic Gels for Biological Use. *Nature 1960 185:4706*, *185*, 117–118.

[28] **Wu, M., Chen, J., Huang, W., Yan, B., Peng, Q., Liu, J., Chen, L., & Zeng, H.** (2020). Injectable and Self-Healing Nanocomposite Hydrogels with Ultrasensitive pH-Responsiveness and Tunable Mechanical Properties: Implications for Controlled Drug Delivery. *Biomacromolecules*, *21*, 2409–2420.

[29] **Tran, N. P. D., & Yang, M. C.** (2019). Synthesis and Characterization of Silicone Contact Lenses Based on TRIS-DMA-NVP-HEMA Hydrogels. *Polymers*, 11, 944.

[30] **Ramachandran, R., Jung, D., & Spokoyny, A. M.** (2019). Cross-linking dots on metal oxides. *NPG Asia Mater*, *11*.

[31] **Mougin, A., Repain, V., Ferre, J., Jamet, J. P., Gierak, J., Mailly, D., Chappert, C., Mathet, V., Warin, P., Chapman, J. N., Magn, T., Terris, D., Folks, L., Weller, D., E Baglin, J. E., Kellock, A. J., Rothui-zen, H., … Gong Presto, J. P.** (2003). Double-Network Hydrogels with Extremely High Mechanical Strength. *Advanced Materials*, *15*, 1155–1158.

[32] **Okay, O., & Oppermann, W.** (2007). Polyacrylamide-clay nanocomposite hydrogels: Rheological and light scattering characterization. *Macromolecules*, *40*, 3378–3387.

[33] **Feng, L., Jia, S. S., Chen, Y., & Liu, Y.** (2020). Highly Elastic Slide-Ring Hydrogel with Good Recovery as Stretchable Supercapacitor. *Chemistry*, *26*, 14080–14084.

[34] **Huang, T., Xu, H., Jiao, K., Zhu, L., Brown, H. R., Wang, H., Wang, H. L., Huang, T., Xu, H. G., Jiao, K. X., Zhu, L. P., & Brown, R.** (2007). A Novel Hydrogel with High Mechanical Strength: A Macromolecular Microsphere Composite Hydrogel. *Advanced Materials*, *19*, 1622–1626.

[35] **Zhao, S. X., & Zhao, X.** (2014). Multi-scale multi-mechanism design of tough hydrogels: building dissipation into stretchy networks. *Soft Matter*, *10*, 672–687.

[36] **Ross-Murphy, S. B.** (1991). Physical Gelation of Synthetic and Biological Macromolecules. *Polymer Gels*, 21–39.

[37] **Brown, H. R.** (2007). A model of the fracture of double network gels. *Macromolecules*, *40*, 3815–3818.

[38] **Ahagon, A., & Gent, A. N.** (1975). Threshold fracture energies for elastomers. *Journal of Polymer Science: Polymer Physics Edition*, *13*, 1903–1911.

[39] **Norioka, C., Inamoto, Y., Hajime, C., Kawamura, A., & Miyata, T.** (2021). A universal method to easily design tough and stretchable hydrogels. *NPG Asia Mater*, *13*.

[40] **Asanuma, H., Ban, T., Gotoh, S., Hishiya, T., & Komiyama, M.** (1998). Hydrogen bonding in water by poly(vinyldiaminotriazine) for the molecular recognition of nucleic acid bases and their derivatives. *Macromolecules*, *31*, 371–377.

[41] **Wang, P., Zhang, J., Li, Y., Wang, N., & Liu, W.** (2015). A nucleoside responsive diaminotriazine-based hydrogen bonding strengthened hydrogel. *Mater. Lett.*, *142*, 71–74.

[42] **Sijbesma, R. P., Beijer, F. H., Brunsveld, L., Folmer, B. J. B., Hirschberg, J. H. K. K., Lange, R. F. M., Lowe, J. K. L., & Meijer, E. W.** (1997). Reversible Polymers Formed from Self-Complementary Monomers Using Quadruple Hydrogen Bonding. *Science (1979)*, *278*, 1601–1604.

[43] **You, Y., Yang, J., Zheng, Q., Wu, N., Lv, Z., & Jiang, Z.** (2020). Ultra-stretchable hydrogels with hierarchical hydrogen bonds. *Scientific Reports 2020 10:1*, *10*, 1–8.

[44] **Hu, X., Vatankhah-Varnoosfaderani, M., Zhou, J., Li, Q., & Sheiko, S. S.** (2015). Weak Hydrogen Bonding Enables Hard, Strong, Tough, and Elastic Hydrogels. *Adv. Mater.*, *27*, 6899–6905.

[45] **Zhang, X. N., Wang, Y. J., Sun, S., Hou, L., Wu, P., Wu, Z. L., & Zheng, Q.** (2018). A Tough and Stiff Hydrogel with Tunable Water Content and Mechanical Properties Based on the Synergistic Effect of Hydrogen Bonding and Hydrophobic Interaction. *Macromolecules*, *51*, 8136–8146.

[46] **Haag, S. L., & Bernards, M. T.** (2017). Polyampholyte Hydrogels in Biomedical Applications. *Gels*, *3*.

[47] **Zurick, K. M., & Bernards, M.** (2014). Recent biomedical advances with polyampholyte polymers. *J. Appl. Polym. Sci.*, *131*, 40069.

[48] **Sun, T. L., Kurokawa, T., Kuroda, S., Ihsan, A. bin, Akasaki, T., Sato, K., Haque, M. A., Nakajima, T., & Gong, J. P.** (2013). Physical hydrogels composed of polyampholytes demonstrate high toughness and viscoelasticity. *Nature Materials 2013 12:10*, *12*, 932–937.

[49] **Ihsan, A. bin, Sun, T. L., Kurokawa, T., Karobi, S. N., Nakajima, T., Nonoyama, T., Roy, C. K., Luo, F., & Gong, J. P.** (2016). Self-Healing Behaviors of Tough Polyampholyte Hydrogels. *Macromolecules*, *49*, 4245–4252.

[50] **Zhang, Y., Hu, Q., Yang, S., Wang, T., Sun, W., & Tong, Z.** (2021). Unique self-reinforcing and rapid self-healing polyampholyte hydrogels with a ph-induced shape memory effect. *Macromolecules*, *54*, 5218–5228.

[51] **Zhang, Y., Liao, J., Wang, T., Sun, W., Tong, Z., Zhang, Y., Liao, J., Wang, T., Sun, W., & Tong, Z.** (2018). Polyampholyte Hydrogels with pH Modulated Shape Memory and Spontaneous Actuation. *Adv. Funct. Mater.*, *28*, 1707245.

[52] **Abdurrahmanoglu, S., Cilingir, M., & Okay, O.** (2011). Dodecyl methacrylate as a crosslinker in the preparation of tough polyacrylamide hydrogels. *Polymer*, *52*, 694–699.

[53] **Tuncaboylu, D. C., Sari, M., Oppermann, W., & Okay, O.** (2011). Tough and self-healing hydrogels formed via hydrophobic interactions. *Macromolecules*, *44*, 4997–5005.

[54] **Tuncaboylu, D. C., Sahin, M., Argun, A., Oppermann, W., & Okay, O.** (2012). Dynamics and large strain behavior of self-healing hydrogels with and without surfactants. *Macromolecules*, *45*, 1991–2000.

[55] **Tuncaboylu, D. C., Argun, A., Sahin, M., Sari, M., & Okay, O.** (2012). Structure optimization of self-healing hydrogels formed via hydrophobic interactions. *Polymer, 53*, 5513–5522.

[56] **Tuncaboylu, D. C., Argun, A., Algi, M. P., & Okay, O.** (2013). Autonomic self-healing in covalently crosslinked hydrogels containing hydrophobic domains. *Polymer, 54*, 6381–6388.

[57] **Baskan, T., Tuncaboylu, D. C., & Okay, O.** (2013). Tough interpenetrating Pluronic F127/polyacrylic acid hydrogels. *Polymer, 54*, 2979–2987.

[58] **Akay, G., Hassan-Raeisi, A., Tuncaboylu, D. C., Orakdogen, N., Abdurrahmanoglu, S., Oppermann, W., & Okay, O.** (2013). Self-healing hydrogels formed in catanionic surfactant solutions. *Soft Matter*, *9*, 2254–2261.

[59] **Bilici, C., & Okay, O.** (2013). Shape memory hydrogels via micellar copolymerization of acrylic acid and n-octadecyl acrylate in aqueous media. *Macromolecules*, *46*, 3125–3131.

[60] **Gulyuz, U., & Okay, O.** (2013). Self-healing polyacrylic acid hydrogels. *Soft Matter*, *9*, 10287–10293.

[61] **Argun, A., Algi, M. P., Tuncaboylu, D. C., & Okay, O.** (2014). Surfactant-induced healing of tough hydrogels formed via hydrophobic interactions. *Colloid Polym. Sci.*, *292*, 511–517.

[62] **Algi, M. P., & Okay, O.** (2014). Highly stretchable self-healing poly(N,N-dimethylacrylamide) hydrogels. *Eur. Polym. J.*, *59*, 113–121.

[63] **Gulyuz, U., & Okay, O.** (2014). Self-healing poly(acrylic acid) hydrogels with shape memory behavior of high mechanical strength. *Macromolecules*, *47*, 6889–6899.

[64] **Akca, O., Yetiskin, B., & Okay, O.** (2020). Hydrophobically modified nanocomposite hydrogels with self-healing ability. *J. Appl. Polym. Sci.* 137(28), 48853.

[65] **Toleutay, G., Su, E., Kudaibergenov, S., & Okay, O.** (2020). Highly stretchable and thermally healable polyampholyte hydrogels via hydrophobic modification. *Colloid Polym. Sci.*, *298*, 273–284.

[66] **Lee, B. P., Messersmith, P. B., Israelachvili, J. N., & Waite, J. H.** (2011). Mussel-Inspired Adhesives and Coatings. *Annu. Rev. Mater. Res.*, *41*, 99–132.

[67] **Fullenkamp, D. E., He, L., Barrett, D. G., Burghardt, W. R., & Messersmith, P. B.** (2013). Mussel-inspired histidine-based transient network metal coordination hydrogels. *Macromolecules*, *46*, 1167–1174.

[68] **Menyo, M. S., Hawker, C. J., & Waite, J. H.** (2013). Versatile tuning of supramolecular hydrogels through metal complexation of oxidation-resistant catechol-inspired ligands. *Soft Matter*, *9*, 10314–10323.

[69] **Barrett, D. G., Fullenkamp, D. E., He, L., Holten-Andersen, N., Lee, K. Y. C., & Messersmith, P. B.** (2013). pH-Based Regulation of Hydrogel Mechanical Properties Through Mussel-Inspired Chemistry and Processing. *Adv. Funct. Mater.*, *23*, 1111.

[70] **Lee, B. P., & Konst, S.** (2014). Novel Hydrogel Actuator Inspired by Reversible Mussel Adhesive Protein Chemistry. *Advanced Materials*, *26*, 3415–3419.

[71] **Krogsgaard, M., Hansen, M. R., & Birkedal, H.** (2014). Metals & polymers in the mix: fine-tuning the mechanical properties & color of self-healing mussel-inspired hydrogels. *J. Mater. Chem. B*, *2*, 8292–8297.

[72] **Li, Q., Barrett, D. G., Messersmith, P. B., & Holten-Andersen, N.** (2016). Controlling hydrogel mechanics via bio-inspired polymer-nanoparticle bond dynamics. *ACS Nano*, *10*, 1317–1324.

[73] **Zeng, L., Song, M., Gu, J., Xu, Z., Xue, B., Li, Y., & Cao, Y.** (2019). A Highly Stretchable, Tough, Fast Self-Healing Hydrogel Based on Peptide–Metal Ion Coordination. *Biomimetics*, *4*.

[74] **Shabbir, H., Dellago, C., & Hartmann, M. A.** (2019). A High Coordination of Cross-Links Is Beneficial for the Strength of Cross-Linked Fibers. *Biomimetics*, *4*.

[75] **Liang, L., Shen, J. W., & Wang, Q.** (2017). Molecular dynamics study on DNA nanotubes as drug delivery vehicle for anticancer drugs. *Colloids Surf B Biointerfaces*, *153*, 168–173.

[76] **Mehra, N. K., & Palakurthi, S.** (2016). Interactions between carbon nanotubes and bioactives: a drug delivery perspective. *Drug Discov. Today*, *21*, 585–597.

[77] **Liu, J., Dong, J., Zhang, T., & Peng, Q.** (2018). Graphene-based nanomaterials and their potentials in advanced drug delivery and cancer therapy. *J. Control Release*, *286*, 64–73.

[78] **Shim, G., Kim, M. G., Park, J. Y., & Oh, Y. K.** (2016). Graphene-based nanosheets for delivery of chemotherapeutics and biological drugs. *Adv. Drug Deliv. Rev.*, *105*, 205–227.

[79] **Loh, K. P., Bao, Q., Ang, P. K., & Yang, J.** (2010). The chemistry of graphene. *J. Mater. Chem.*, *20*, 2277–2289.

[80] **Li, F., Zhu, Y., You, B., Zhao, D., Ruan, Q., Zeng, Y., & Ding, C.** (2010). Smart Hydrogels Co-switched by Hydrogen Bonds and π–π Stacking for Continuously Regulated Controlled-Release System. *Adv. Funct. Mater.*, *20*, 669–676.

[81] **Szejtli, J.** (1998). Introduction and general overview of cyclodextrin chemistry. *Chem. Rev.*, *98*, 1743–1753.

[82] **Rodell, C. B., Kaminski, A. L., & Burdick, J. A.** (2013). Rational design of network properties in guest-host assembled and shear-thinning hyaluronic acid hydrogels. *Biomacromolecules*, *14*, 4125–4134.

[83] **Guan, Y., Zhao, H. B., Yu, L. X., Chen, S. C., & Wang, Y. Z.** (2014). Multi-stimuli sensitive supramolecular hydrogel formed by host–guest interaction between PNIPAM-Azo and cyclodextrin dimers. *RSC Adv.*, *4*, 4955–4959.

[84] **Mun, G., Suleimenov, I., Park, K., & Omidian, H.** (2010). Superabsorbent Hydrogels. *Biomedical Applications of Hydrogels Handbook*, 375–391.

[85] **Santos, R. V. A., Costa, G. M. N., & Pontes, K. v.** (2019). Development of Tailor-Made Superabsorbent Polymers: Review of Key Aspects from Raw Material to Kinetic Model. *J. Polym. Environ.*, *27*, 1861–1877.

[86] **Askari, F., Nafisi, S., Omidian, H., & Hashemi, S. A.** (1993). Synthesis and characterization of acrylic-based superabsorbents. *J. Appl. Polym. Sci.*, *50*, 1851–1855.

[87] **Omidian, H., Hashemi, S. A., Sammes, P. G., & Meldrum, I.** (1999). Modified acrylic-based superabsorbent polymers (dependence on particle size and salinity). 40, 1753–1761.

[88] **Wack, H., & Ulbricht, M.** (2007). Method and model for the analysis of gel-blocking effects during the swelling of polymeric hydrogels. *Ind. Eng. Chem. Res.*, *46*, 359–364.

[89] **Arlit, D., Glabisch, D., aden, O., & Suling, C.** (1969). Polymers containing sulphonic acid groups. *a corporation of Germany No Drawing. Continuation of application Ser*, *233*.

[90] **Nalampang, K., Molloy, R., Mai Sci, C. J., Suebsanit, N., & Witthayaprapakorn, C.** (2007). *Design and Preparation of AMPS-Based Hydrogels for Biomedical Use as Wound Dressings*. *Chiang Mai J. Sci* (Vol. 34). Retrieved from www.science.cmu.ac.th/journal-science/josci.html

[91] **Xing, X., Li, L., Wang, T., Ding, Y., Liu, G., & Zhang, G.** (2014). A self-healing polymeric material: from gel to plastic. *J. Mater. Chem. A Mater.*, *2*, 11049–11053.

[92] **Su, E., & Okay, O.** (2018). Hybrid cross-linked poly(2-acrylamido-2-methyl-1-propanesulfonic acid) hydrogels with tunable viscoelastic, mechanical and self-healing properties. *React. Funct. Polym.*, *123*, 70–79.

[93] **Kazantsev, O. A., Igolkin, A. v., Shirshin, K. v., Kuznetsova, N. A., Spirina, A. N., & Malyshev, A. P.** (2002). Spontaneous polymerization of 2-acrylamido-2-methylpropanesulfonic acid in acidic aqueous solutions. *Russian Journal of Applied Chemistry*, *75*, 465–469.

[94] **Erkoc, C., Yildirim, E., Yurtsever, M., & Okay, O.** (2022). Roadmap to Design Mechanically Robust Copolymer Hydrogels Naturally Cross-Linked by Hydrogen Bonds. *Macromolecules*, *55*, 10576–10589.

[95] **Cipriano, B. H., Banik, S. J., Sharma, R., Rumore, D., Hwang, W., Briber, R. M., & Raghavan, S. R.** (2014). Superabsorbent hydrogels that are robust and highly stretchable. *Macromolecules*, *47*, 4445–4452.

[96] **Song, G., Zhang, L., He, C., Fang, D.-C., Whitten, P. G., & Wang, H.** (2013). Facile Fabrication of Tough Hydrogels Physically Cross-Linked by Strong Cooperative Hydrogen Bonding. *Macromolecules, 46(18),* 7423–7435.

[97] **Kříž, J., Dybal, J., & Brus, J.** (2006). Cooperative hydrogen bonds of macromolecules. 2. Two-dimensional cooperativity in the binding of poly(4-vinylpyridine) to poly(4-vinylphenol). *Journal of Physical Chemistry B*, *110*, 18338–18346.

[98] **Říž, J., & Dybal, J.** (2007). Cooperative hydrogen bonds of macromolecules. 3. A model study of the proximity effect. *Journal of Physical Chemistry B*, *111*, 6118–6126.

[99] **Kauzman, W., & Eyring, H.** (1940). The Viscous Flow of Large Molecules. *J. Am. Chem. Soc.*, *62*, 3113–3125.

[100] **Sweeney, J., & Ward, I.** (2012). *Mechanical properties of solid polymers*, John Wiley & Sons.

[101] **McCrum, N., Buckley, C., Buckley, C., & Bucknall, C.** (1997). *Principles of polymer engineering*, University Press, Oxford.

[102] **Ward, I. M.** (1971). Review: The yield behaviour of polymers. *J. Mater. Sci*., 6, 1397-1417.

[103] **Kurt, B., Gulyuz, U., Demir, D. D., & Okay, O.** (2016). High-strength semi-crystalline hydrogels with self-healing and shape memory functions. *Eur. Polym. J.*, *81*.

[104] **Bilici, C., Ide, S., & Okay, O.** (2017). Yielding Behavior of Tough Semicrystalline Hydrogels. *Macromolecules*, *50*.

[105] **Uzumcu, A. T., Guney, O., & Okay, O.** (2018). Highly Stretchable DNA/Clay Hydrogels with Self-Healing Ability. *ACS Appl. Mater. Interfaces*, *10*, 8296–8306.

[106] **Topuz, F., & Okay, O.** (2009). Macroporous hydrogel beads of high toughness and superfast responsivity. *React. Funct. Polym.*, *69*, 273–280.

APPENDIX

Table A.1 : The swelling ratio and mechanical parameters of the hydrogels prepared at various x_{MAAc}. w = 25 wt%. Standard deviations are provided in brackets.

x_{MAAc}	m_{rel}	E / MPa	σ_f / MPa	ε_f %	W / MJ.m^{-3}
1.0	1400 (303)	5.3 (0.6)	4.0 (0.2)	316 (25)	11.9 (1.7)
0.8	2035 (255)	26.1 (1.5)	10.4 (0.7)	325 (42)	30.8 (2.9)
0.7	2063 (154)	23.2 (3.4)	10.7 (0.5)	237 (52)	26.9 (1.4)
0.6	2913 (134)	11.2 (2.1)	7.4 (0.8)	416 (46)	24.0 (2.2)
0.5	2613 (193)	10.5 (1.3)	7.1 (0.4)	703 (55)	44.4 (4.8)
0.4	2200 (15)	2.17 (0.2)	2.5 (0.3)	633 (50)	13.5 (1.5)
0.2	1710 (76)	1.12 (0.1)	1.2 (0.1)	388 (23)	4.5 (0.3)
0.0	1071 (75)	0.40 (0.05)	0.58 (0.05)	329 (30)	2.0 (0.4)

Table A.2 : The mechanical parameters of the hydrogels prepared at various w. x_{MAAc} = 0.80. Standard deviations are provided in brackets.

w %	E / MPa	σ_f / MPa	ε_f %	W / MJ.m^{-3}
25	26.1 (1.5)	10.4 (0.7)	325 (42)	30.8 (2.9)
30	1.6 (0.1)	2.2 (0.2)	517 (44)	8.7 (0.9)
40	0.36 (0.03)	0.30 (0.02)	249 (13)	0.72 (0.14)
50	0.17 (0.01)	0.12 (0.01)	169 (12)	0.18 (0.02)
75	7×10^{-3} (1×10^{-3})	0.015 (0.001)	456 (39)	0.063 (0.005)
80	7×10^{-3}	--	--	--

Table A.3 : Elemental microanalysis results of sol and gel phases of the hydrogels prepared at w = 93 and 95 wt%.

Location	w wt%	C wt%	N wt%	S wt%
Sol	95	42	5.74	8.7
	93	42.4	5.87	9.21
Gel	95	48.9	2.98	3.77
	93	45.9	4.41	6.36
In the feed		47.3	5.3	9.1

Table A.4 : The composition of sol and gel phases of the hydrogels prepared at w = 95 and 93 wt%.

Location	w wt%	AMPS mol%	DMAA mol%	MAAc mol%	x_{MAAc}
Sol	95	35.8	18.2	46.0	0.72
	93	38.9	17.9	43.2	0.71
Gel	95	12.0	9.7	78.3	0.89
	93	22.9	13.5	63.6	0.83
In the feed		38	12.4	49.6	0.80

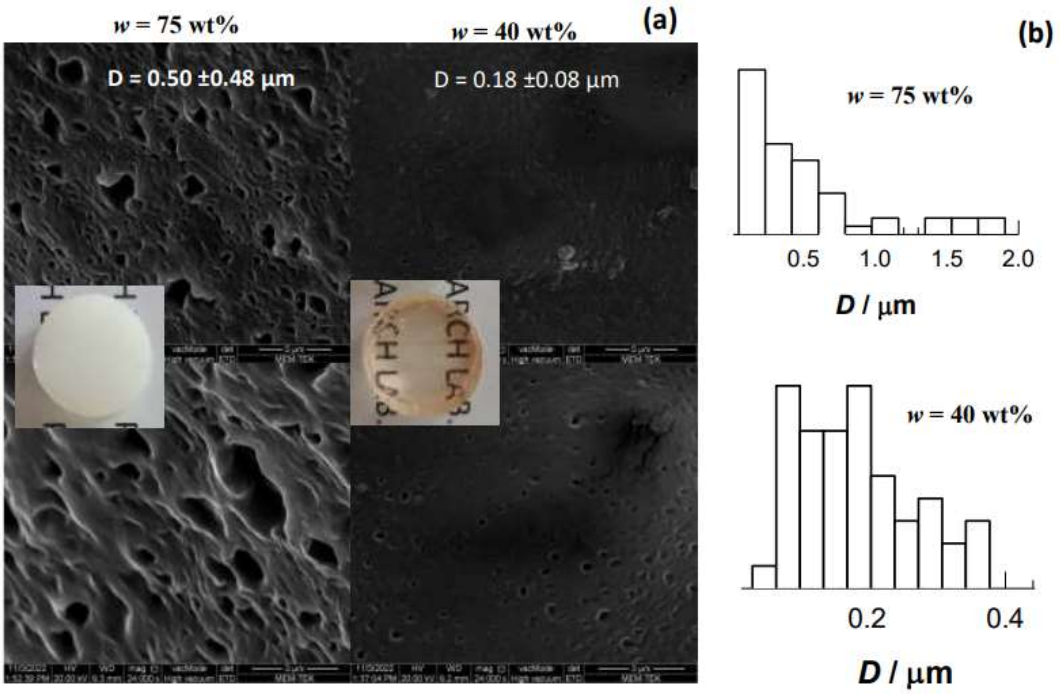

Figure A.1 : (a) SEM images of freeze-dried terpolymer hydrogels formed at w = 75 and 40 wt% as stated. Scale bars are 5 (up) and 3 µm (bottom). The inset to the SEM images presents the optical images of the hydrogels. (b) The pore size distribution for the same terpolymers, and the average pore diameters estimated by analyzing at least 50 pores in the images taken at various magnifications.

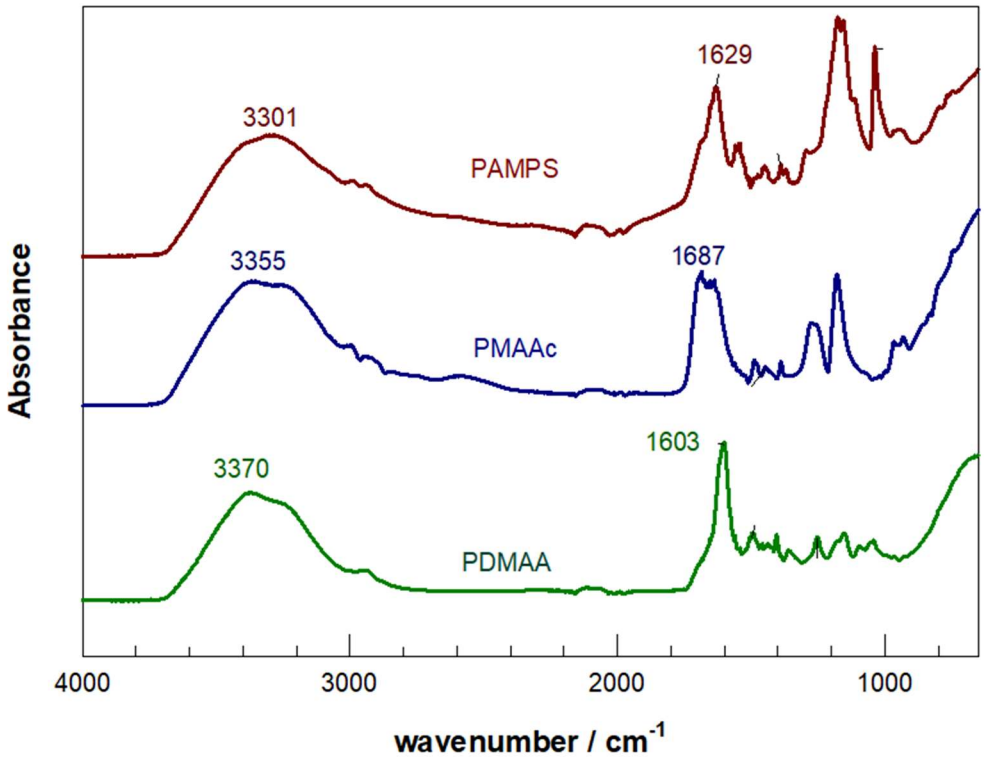

Figure A.2 : FTIR spectra of PAMPS, PMAAc, and PDMAA physical hydrogels formed at w = 50 wt% under identical conditions as described in the text.

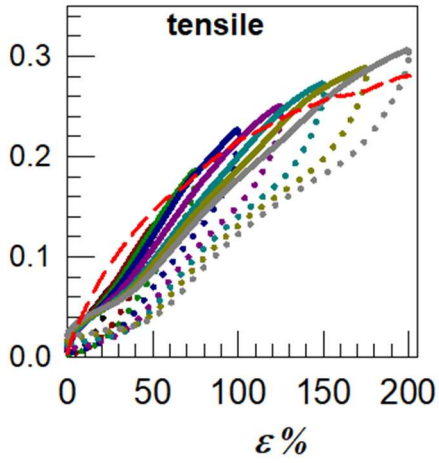

Figure A.3 : Dashed red curve represents the stress-strain curve of the virgin sample (w= 40 wt%).

CURRICULUM VITAE

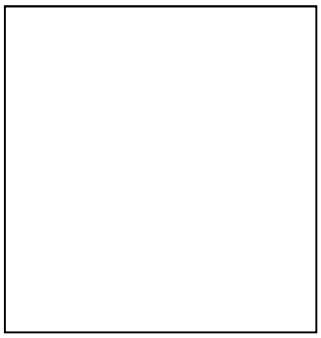

Name Surname **:** Büşra SEKİZKARDEŞ

EDUCATION **:**

- **B.Sc.** **:** 2020, Yıldız Technical University, Faculty of Science and Arts, Chemistry
- **M.Sc.** **:** 2023, Istanbul Technical University, Graduate School, Chemistry

PROFESSIONAL EXPERIENCE:

- Research Assistant, Department of Material Science and Technology, Turkish-German University (2022-still)

PUBLICATIONS ON THE THESIS:

- **Sekizkardeş, B., Su, E., and Okay, O.** (2022). AMPS-Based H-Bonded Superabsorbent Hydrogels, IGRS'22 International Graduate Research Symposium, İstanbul, Turkey. June 1-3.
- **Sekizkardes, B., Su, E., & Okay, O.** (2023). Mechanically Strong Superabsorbent Terpolymer Hydrogels Based on AMPS via Hydrogen-Bonding Interactions, *ACS Applied Polymer Materials*. 5 (3), 2043-2050 https://doi.org/10.1021/acsapm.2c02085